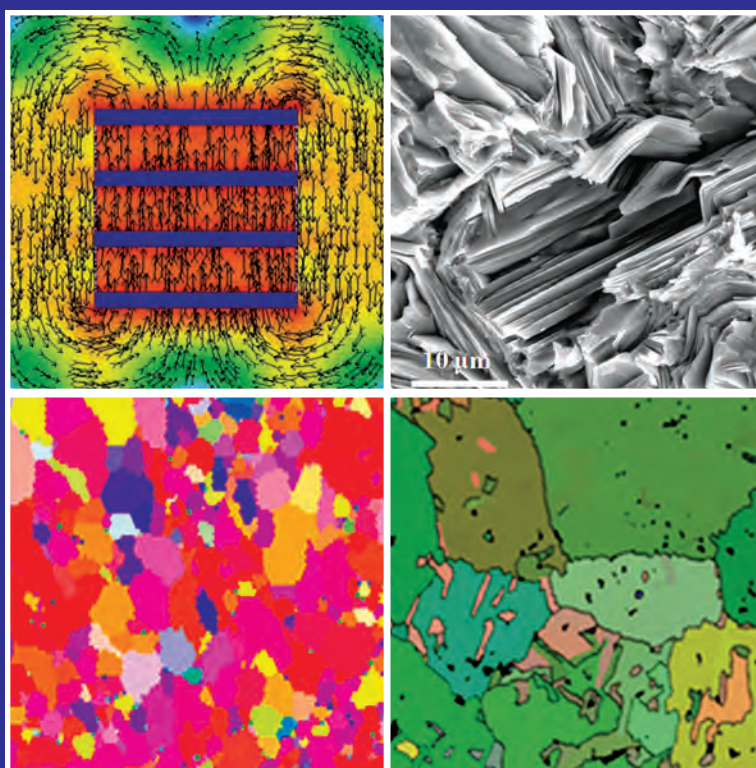


BARC

NEWSLETTER



भाभा परमाणु अनुसंधान केंद्र
BHABHA ATOMIC RESEARCH CENTRE



IN THIS ISSUE

- Prompt Identification of Tsunamigenic Earthquakes from Multi-Station Seismic Data
- Phase Transformation and Deformation Studies in Zr Based Alloys
- Assessment of Higher Order Shear and Normal Deformations Theories for Stress Analysis and Free Vibration of Functionally Graded Plates
- The elusive neutrino
- Seamless Access to Networked Information: The Role of Domain Ontologies

In the Forthcoming Issue

1. Multiple diglycolamide functionalized ligands in room temperature ionic liquids: 'green' solvents for actinide partitioning
Arijit Sengupta et al.
2. Design, Development and Commercialization of *ISOCAD* (Integrated System Of Computer Aided Dosimetry) for gamma irradiators
Amit Shrivastava et al.
3. Delayed Time Response Self-Powered Neutron Detectors for Reactor Control
A. Mishra et al.
4. Photosensitization of skin cancer cells, by coralyne, is mediated through ATR-p38 MAPK-Bax and JAK2-STAT1-BAX pathways
Rahul Bhattacharyya et al.
5. Drop-Interface Coalescence in Liquid-Liquid systems: Effect of surface active agents
Smita Dixit, et al.

CONTENTS

<i>Editorial Note</i>	ii
Brief Communications	
• Lutetium-177 Labeled Hydroxyapatite (HA) for the Treatment of Rheumatoid Arthritis: Kit Product Development	iii
• High Figure-of-Merit Thermoelectric Materials	iv
Research Articles	
• Prompt Identification of Tsunamigenic Earthquakes from Multi-Station Seismic Data <i>A.K.Pal, et al.</i>	1
• Phase Transformation and Deformation Studies in Zr Based Alloys <i>K.V. Mani Krishna, D. Srivastava and G.K. Dey</i>	8
• Assessment of Higher Order Shear and Normal Deformations Theories for Stress Analysis and Free Vibration of Functionally Graded Plates <i>D.K. Jha, et al.</i>	13
Feature Articles	
• The elusive neutrino <i>V.M. Datar</i>	22
• Seamless Access to Networked Information: The Role of Domain Ontologies <i>Sangeeta Deokattey and K. Bhanumurthy</i>	31
News and Events	
• Theme Meeting on Challenges in Fast Reactor Fuel Reprocessing (CFRR-2014)	38
• Technology Transfer to Industries	39
• Honour for BARC	43
BARC Scientists Honoured	44

Editorial Committee

Chairman

Dr. S.K. Apte,
Director, Bio-Science Group

Editor

Dr. K. Bhanumurthy
Head, SIRD

Associate Editors for this issue

Dr. G. Rami Reddy, RSD
Dr. A.K. Naik, RED

Members

Dr. R.C. Hubli, MPD
Dr. D.N. Badodkar, DRHR
Dr. K.T. Shenoy, ChED
Dr. A.P. Tiwari, RCnD
Dr. S.M. Yusuf, SSPD
Dr. A.K. Tyagi, ChD
Mr. G. Venugopala Rao, APPD
Dr. C.P. Kaushik, WMD
Dr. G. Rami Reddy, RSD
Dr. S. Kannan, FCD
Dr. A.K. Nayak, RED
Dr. S.K. Sandur, RB&HSD
Dr. S.C. Deokattey, SIRD

From the Editor's Desk.....

Welcome to the September-October 2014 issue of the BARC Newsletter. It features five articles, Two Brief Communications and reports of various scientific events organized by BARC.

One of the articles showcases R&D work (which received the INSA Young Scientist Honour) on microstructural and textural changes, taking place during the processing of the Zirconium alloys and their role in the hydriding behavior. Zirconium-based structural components are an integral part of thermal nuclear reactors.

The second article is on Functionally Graded Materials (FGMs), which are recent additions to the family of engineering composites made of two or more constituent phases. These materials are used for making nuclear components. Stress analysis and free vibration of FG elastic, rectangular and simply (diaphragm) supported plates are discussed in the article.

Under-sea earthquakes have the deadly potential of generating Tsunamis. Quick determination of hypocenter, magnitude and fault plane parameters of these earthquakes is essential in assessing the tsunami generating potential of these earthquakes. The article discusses an in-house software that has been developed to analyze various parameters from the seismic waveform data recorded at global stations available over the internet.

A feature article on Neutrinos throws light on the elementary particle, its various sources and the Indian effort to build an underground laboratory; the India-based Neutrino Observatory (INO).

Another feature article discusses the role of domain ontologies, (which are semantic networks of interconnected concepts on various subject domains), in providing seamless access to networked information and R&D efforts at BARC in this direction.



Dr. K. Bhanumurthy
On behalf of the Editorial Committee

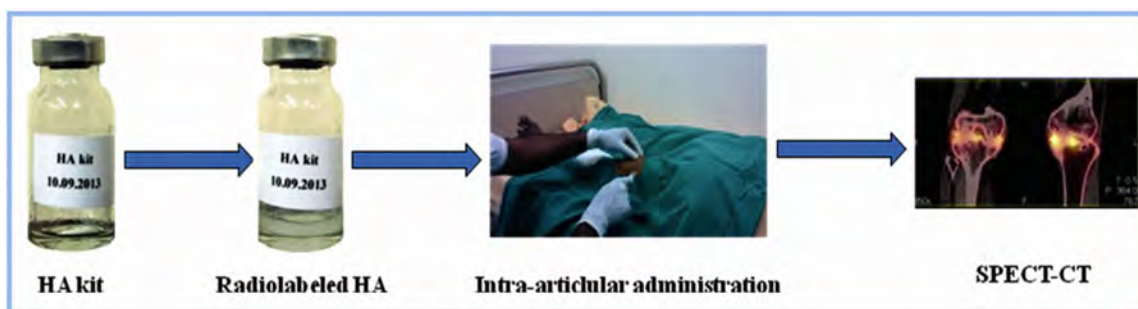
Lutetium-177 Labeled Hydroxyapatite (HA) for the Treatment of Rheumatoid Arthritis: Kit Product Development

Radiochemistry and Isotope Group

Intra-articular administration of particulate formulations of β^- emitting radionuclides of suitable decay properties is a treatment option for patients suffering from inflammatory joint disorders like rheumatoid arthritis (RA) to relieve pain and inflammation, the procedure being known as 'radiation synovectomy'. BARC has developed and made available products for this purpose using different radionuclides. Among these, the use of ^{177}Lu [$T_{1/2} = 6.65$ d, $E_{\beta(\text{max})} = 497$ keV, $E_{\gamma} = 113$ KeV (6.4%), 208 KeV (11%)] is attractive, especially for medium-size joints, owing to its β^- decay energy as well as easy and cost-effective production using Dhruva reactor. In view of this, the Isotope Production & Applications Division (formerly Radiopharmaceuticals Division) has developed a ready-to-use kit containing hydroxyapatite particles (HA, 1-10 μm size, that had been used in the past

for similar application with other radionuclides) for formulation of ^{177}Lu -labeled HA at the hospital radiopharmacy for subsequent clinical use. Following *in vitro* radiochemical studies and pre-clinical evaluation in animal models done by IPAD-BARC, Kovai Medical Center & Hospital, Coimbatore performed the first clinical application of the product in RA patients. Their clinical study had been approved by the institutional ethics committee (Registration No ECR/112/INST/TN/2013) and all patients had provided written informed consent. Significant improvement was reported in ten patients with rheumatoid arthritis of knee joints treated with 333 ± 46 MBq dose of ^{177}Lu -HA.

The BARC-developed kits would enable convenient one-step preparation of ^{177}Lu -HA (400 ± 30 MBq dose) of $>99\%$ radiochemical purity at hospital radiopharmacy for clinical use.



Treatment of rheumatoid arthritis using ^{177}Lu -HA developed at BARC

High Figure-of-Merit Thermoelectric Materials

Physics Group

Thermoelectric power generators (TEG) are gaining importance for the conversion of waste heat (from automobiles, industries, nuclear reactors etc.) directly into electricity. The key parameter for obtaining high conversion efficiency is figure-of-merit i.e. $ZT = (S^2\sigma/k)T$, where S, σ, k , and T are respectively, Seebeck coefficient, electrical conductivity, thermal conductivity and temperature. For a given thermoelectric material, S, σ and k are interdependent and typical ZT is limited to ≤ 1 [1]. One of the effective approaches to maximize ZT is to lower down k without reducing the power factor ($S^2\sigma$), which can be achieved by reducing the lattice contribution of k . Based on this approach, $(\text{AgCrSe}_2)_{0.5}(\text{CuCrSe}_2)_{0.5}$ composites and SiGe materials were synthesized using solid-state reaction and mechanical alloying, respectively. The ZT of $(\text{AgCrSe}_2)_{0.5}(\text{CuCrSe}_2)_{0.5}$ composite was found to be 1.4 (at 773 K), which is far superior as compared to ZT of ~ 1 reported for individual constituents. (The detailed studies of $(\text{AgCrSe}_2)_{0.5}(\text{CuCrSe}_2)_{0.5}$ composites, as shown in Fig.1, revealed that the

composite consists of hierarchical architectures i.e. phonon scattering centers at different length scales, such as, atomic scale disorder, nanoscale amorphous structure, natural grain boundaries due to layered structure and mesoscale grain boundaries/interfaces, which resulted in a drastic reduction of the lattice thermal conductivity [1]). Similarly, the nanostructured SiGe alloy exhibited record ZT of 1.8 (at 1073 K), which is much higher than the previously reported value of 1.4 [3]. Mechanical alloyed SiGe exhibits dislocations, nanosized amorphous precipitates, and mesoscale grain boundaries, which scatter phonons of all wavelengths and hence lowers down the value of k [2]. Use of such tailor made high ZT materials are expected to enhance the efficiency of TEG suitable for directed conversion of heat into electricity

1. S. Bhattacharya et al., *Journal of Materials Chemistry A* 2(2014) 17122-17129
2. R. Basu et al. *Journal of Materials Chemistry A* 2 (2014) 6922-6930
3. S. Bathula et al., *Appl. Phys. Lett.* 101 (2012) 213902

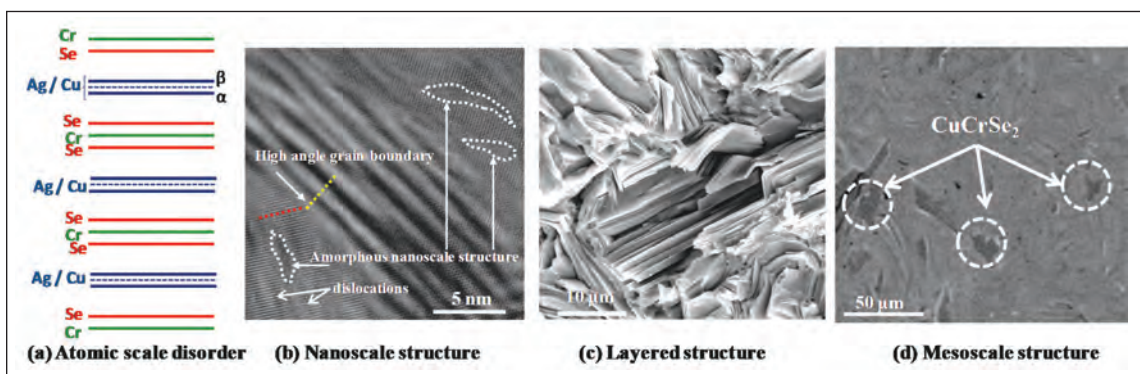


Fig. 1: Hierarchical architectures of $(\text{AgCrSe}_2)_{0.5}(\text{CuCrSe}_2)_{0.5}$ composites

Prompt Identification of Tsunamigenic Earthquakes from Multi-Station Seismic Data

A.K.Pal, A.Kundu, K.K.Bhuyan, A.C.Joy, Y.S.Bhadauria,
A.Vijaya Kumar and S.Mukhopadhyay
Seismology Division

Abstract

Quick determination of hypocenter, magnitude and fault plane parameters of a large undersea earthquake is useful in assessing its tsunami generating potential. An in-house software has been developed to find out these parameters of the earthquake from the near real time seismic waveform data recorded at global stations. Using these parameters vertical displacement of ocean floor is computed which effectively determines the volume of water displaced by the earthquake. Decision logic has been implemented to generate warning based on the computed water volume. Water level data from tide gauge stations near the earthquake source is also monitored to confirm generation of tsunami. At present the software has been developed to monitor earthquakes in the Andaman, Nicobar and Sumatra Regions in Indian Ocean/ Bay of Bengal.

Introduction

Tsunamis are mainly generated by vertical uplift of water from an undersea earthquake. Usually a large earthquake with thrust fault in the oceanic subduction zone generates tsunami. On the other hand large undersea earthquakes with strike-slip fault may not generate appreciable tsunami. For example strike-slip earthquake of 8.6 magnitude in Indian Ocean, which occurred on 11th April, 2012 did not generate significant tsunami. Thus tsunami generation is not only dependent on the earthquake magnitude but also on the type of fault, local bathymetry and earthquake location (latitude, longitude and depth of the hypocenter) [1]. Based on this information, a tsunami warning software (Fig. 1) has been developed, which consists of two modules, one for the estimation of earthquake hypocenter, magnitude and fault plane parameters using global seismic waveform data [2] and the other for the estimation of the displaced volume of water from earthquake using fault plane parameters and local bathymetry near the earthquake hypocenter.

It is well known that fault plane parameters are best estimated using data from seismic stations which are azimuthally distributed around the source. Seismogram Analysis of Global Events (SAGE) module has been developed to estimate the earthquake location, magnitude and fault plane parameters (strike, dip and slip angles) using near real time seismic data (latency about one minute) from the global seismic stations. Earthquake hypocenter location, magnitude and fault parameters are passed on to the tsunami assessment module which determines whether the earthquake is undersea (using global bathymetry data) and computes the volume of water displaced by the earthquake. Depending upon the quantity of the water volume displaced, the tsunami type is categorized as local tsunami, regional tsunami, ocean-wide tsunami or no tsunami. The generation of tsunami is further confirmed using tide gauge monitoring tool which has been developed to monitor the sea level from available tide gauge data from global tide stations.

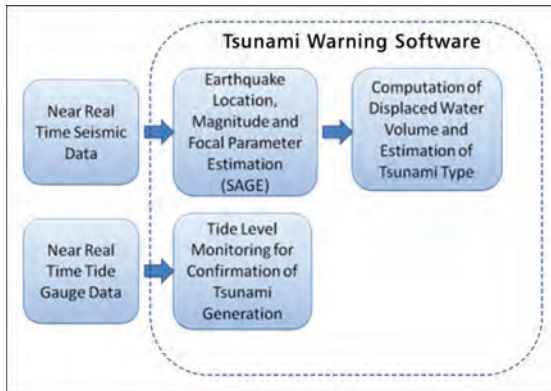


Fig.1: Block diagram of tsunami warning software

Earthquake Fault Parameters

Normally earthquake happens when on a fault one block of rock slips over the other after breaking, due to stress accumulation exceeds the breaking strength of rock. Any earthquake fault plane is defined by three angles [3] as shown in Fig. 2.

- 1) Strike (ϕ): Direction (with respect to North) of a line created by the intersection of a fault plane and a horizontal surface.
- 2) Dip (δ): Angle between the fault plane and the horizontal plane.
- 3) Slip (λ): This is the direction a hanging wall moves during rupture measured on the plane of the fault with respect to horizontal.

In this figure \hat{n} is vector normal to the fault plane and \hat{d} is the slip vector in the fault plane.

Dip (δ) and slip (λ) angles determine the type of fault as depicted in Fig. 3.

A quick and easy method to determine the earthquake fault parameters is by observing primary

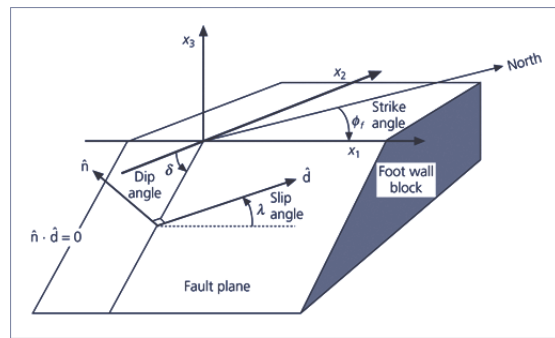


Fig. 2: Earthquake fault plane

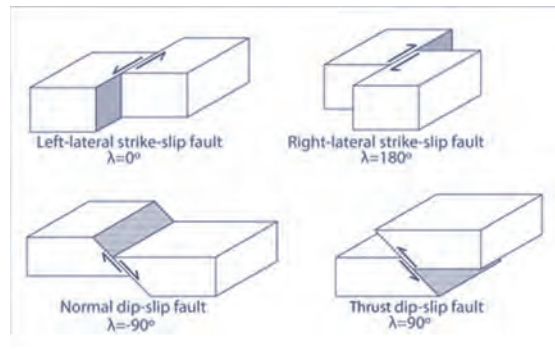


Fig. 3: Type of earthquake faults

wave (P wave) radiation pattern from the first motion polarity of the seismograms recorded at different distances and azimuths around the earthquake epicenter. Depending upon the direction relative to earthquake fault planes the recorded seismogram first motion will be either compression (up) or dilatation (down) as shown in Figs. 4, 5(a) & (b).

Earthquake fault parameters are generally represented by a beach ball diagram, where the first motion in the lower hemisphere of the focal sphere (an imaginary sphere around the earthquake hypocenter which radiates seismic waves all around

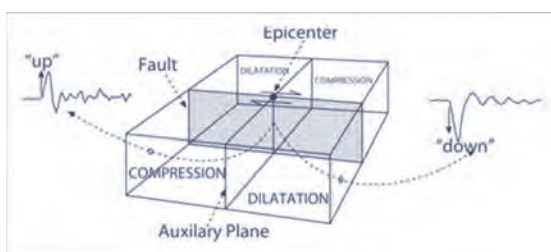


Fig.4: Compression and dilatation motion from earthquake fault

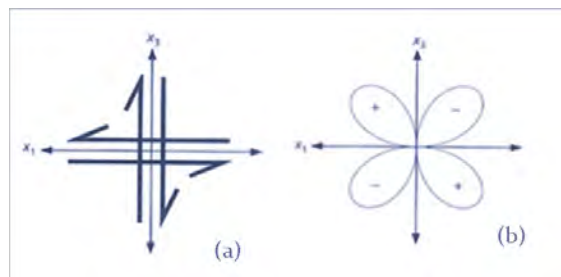


Fig. 5: (a) P wave radiation pattern (b) for two earthquake fault planes

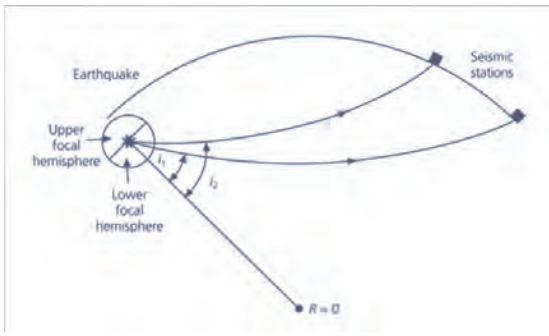


Fig. 6: Earthquake focal sphere

as shown in Fig. 6) is projected on a surface and compression motion is shaded black (dark) and dilatational motion is shaded white (light). Beach ball representations of some common fault types are shown in Fig. 7.

Estimation of Earthquake Location, Magnitude and Fault Parameters

When a large earthquake occurs, data from the stations having a good azimuthal coverage of source region are fetched from Incorporated Research Institutes for Seismology (IRIS) data server [2] using SAGE module. Earthquake location and magnitude are estimated by picking up onset times of Primary (P) and Secondary (S) phases recorded on the seismograms. Body wave magnitude (M_b) is computed from short period P wave amplitude and surface wave magnitude (M_s) is computed from 20 second period Rayleigh (LR) wave which is recorded after P and S waves. However it is well known that both M_b and M_s saturate at around 6.5 and 8 respectively. Hence for large magnitude earthquakes it is preferred to compute moment magnitude as representative of actual energy released by the earthquake. A computation module has also been incorporated in SAGE to compute moment magnitude (M_w) from very long period surface waves using variable period (between 40 and 300 second) mantle magnitude technique introduced by Okal and Talandier [4], [5]. While picking up P wave onset, the polarity of the first motion (either up or down) is also marked on the seismograms. For focal mechanism estimation, a grid search algorithm has been implemented to find the best fitted strike, dip

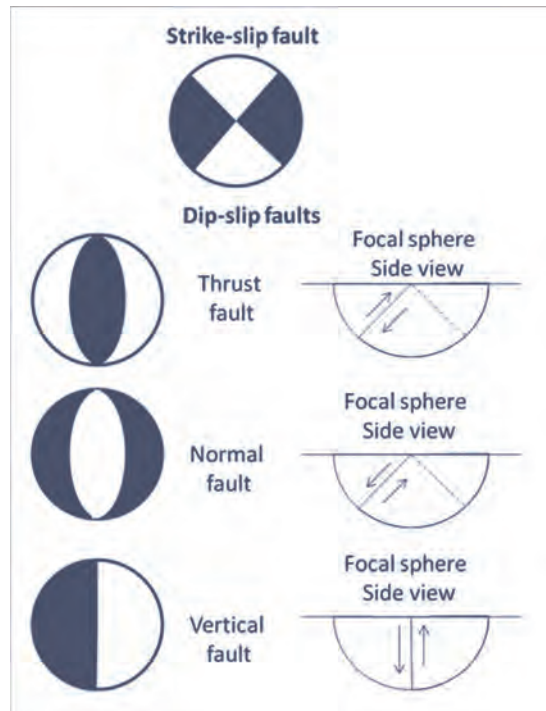


Fig. 7: Representation of earthquake focal mechanism in beach ball plot

and slip values by iteratively comparing the observed P wave radiation pattern with the theoretically computed P wave radiation pattern (Fig. 8). This best fit set of strike, dip and slip values is taken as primary focal plane solution and an additional solution corresponding to auxiliary focal plane is also computed.

Tsunami Warning Based on Earthquake Location, Magnitude and Fault Plane Parameters

After the seismic moment magnitude (M_w) and fault plane parameters are computed, the tsunami category can be found approximately by computing the volume (V_T) of the displaced water at the tsunami source that is approximately equal to the volume of displaced ocean bottom. For a shallow faulting (depth less than 70km) with dip δ and slip λ , volume V_T can be approximately expressed as [6]

$$V_T = \frac{M_0 \sin(\delta) \sin(\lambda)}{\mu} \tag{1}$$

Where M_0 is the seismic moment and μ is the rigidity of the earth crust at the source.

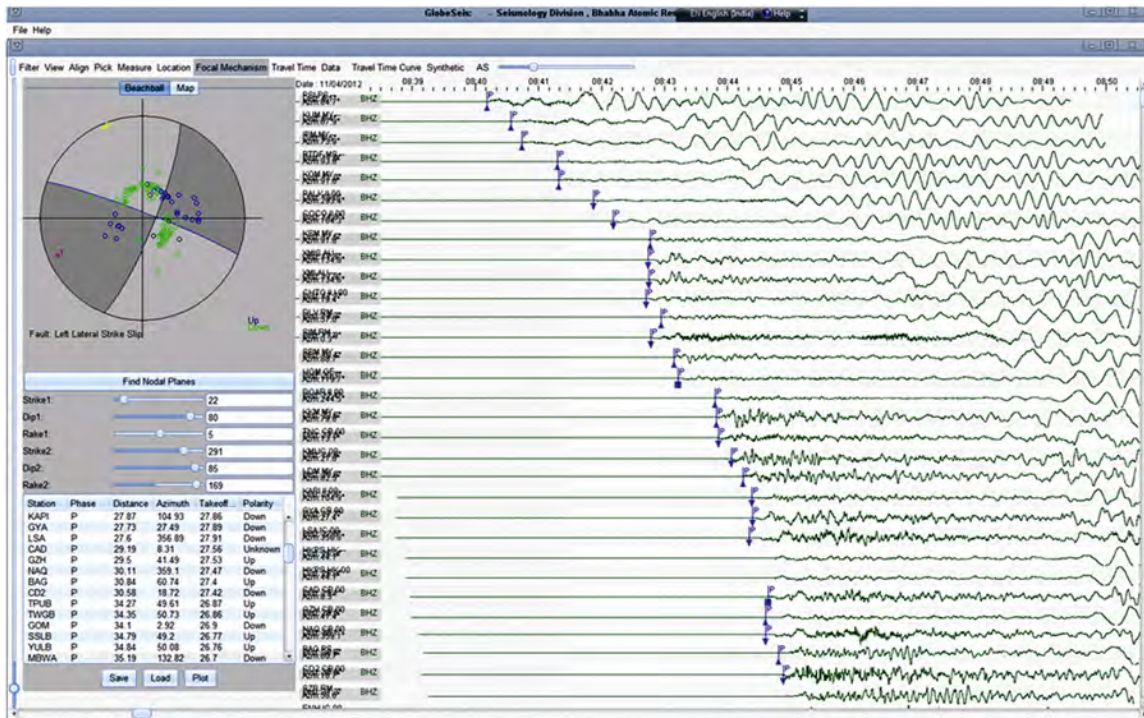


Fig. 8: SAGE module for earthquake focal mechanism, hypocenter location and magnitude estimation.

Note that seismic moment (M_0) is related to moment magnitude by [7]

$$M_W = 0.67 \log(M_0) - 10.7 \quad (2)$$

where, M_0 is in dyne-cm. Using (1) and (2) V_T can be expressed in m^3 as:

$$V_T = \frac{\sin(\delta) \sin(\lambda)}{\mu 10^7} 10^{(Mw + 10.7)/0.67} \quad (3)$$

Using (3) and considering $\mu = 3 \times 10^{10} \text{ N/m}^2$ [6], volume of the displaced water has been computed for a large number of tsunamigenic as well as non-tsunamigenic events that had occurred around the world in the past and whose effects in the regions around the epicenter are well documented [8]. Comparing these water volumes with the reported effects following empirical tsunami category scale, as given in Table 1 has been implemented in the software.

Table 1: Tsunami category scale

$V_T < 1.0 \times 10^8$	No Tsunami
$1.0 \times 10^8 \leq V_T < 1.0 \times 10^9$	Local Tsunami*
$1.2 \times 10^9 \leq V_T < 2.0 \times 10^{10}$	Regional Tsunami **
$V_T \geq 2.0 \times 10^{10}$	Ocean-wide Tsunami ***

* Local Tsunami: Destructive effects are confined to coasts within about 100km of the source.

** Regional Tsunami: Destructive effects are confined to coasts up to about 1000km of the source

*** Ocean-Wide Tsunami: Destructive effects are spread beyond 1000km from the source.

In the tsunami estimation module, before computing the volume of water displaced, it is essential to ascertain whether the earthquake is under the sea. For this water depth above the earthquake hypocenter is estimated using global bathymetry data ETOPO2 [9], which has been incorporated in this module. Another way to confirm the earthquake

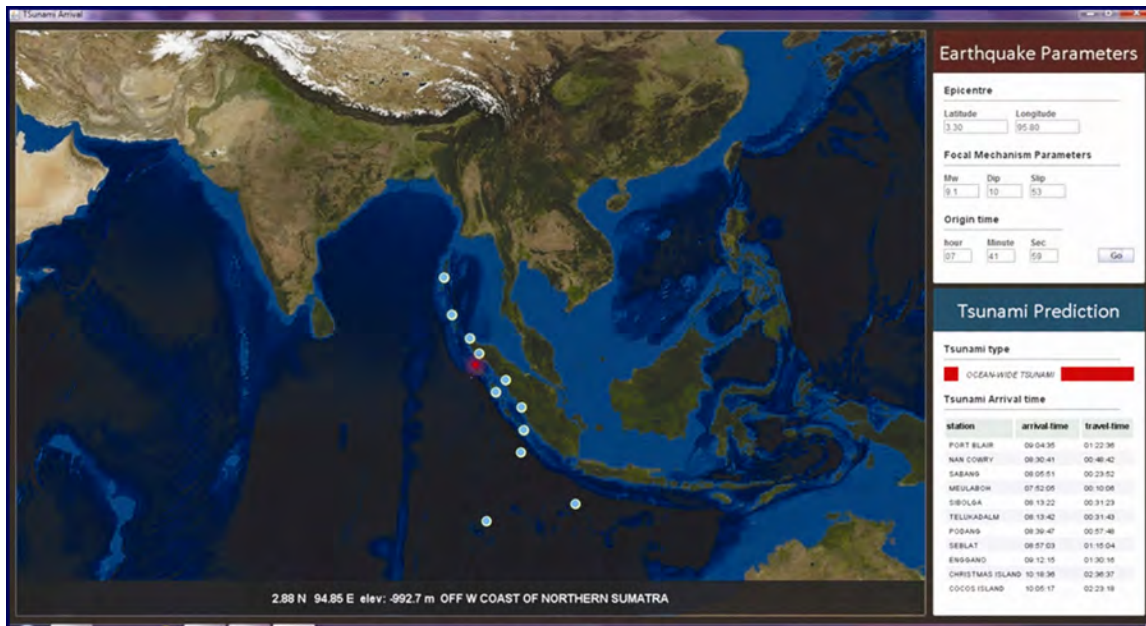


Fig. 9: Tsunami estimation module

as under sea is by observing the presence of Tertiary (T) phase in the seismogram. The T phase travels as short period acoustic wave through the low velocity SOFAR channel in the sea and is recorded at coastal stations after P, S and LR waves. This module also calculates the tentative arrival time of tsunami at

tidal stations located in this region (Fig. 9). An online tide monitoring tool has been developed to acquire and monitor tide gauge data of Sumatra region, Andaman-Nicobar Islands and of Indian Coast (Fig. 10). Brief explanation with figure.

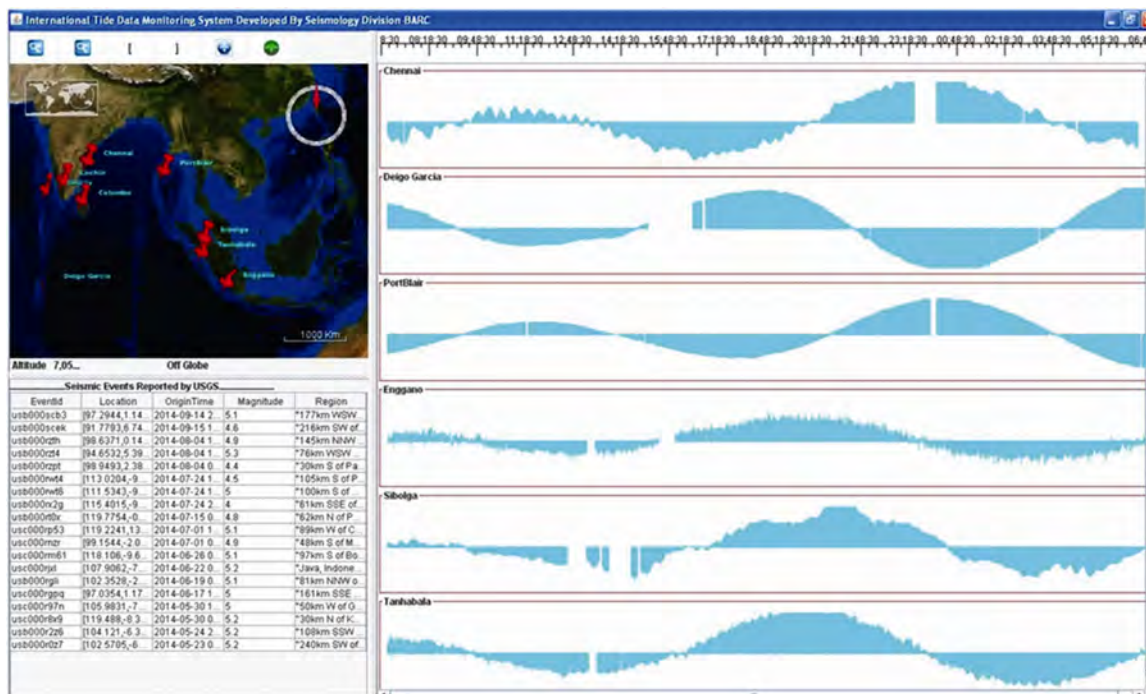


Fig. 10: Online tide gauge monitoring tool

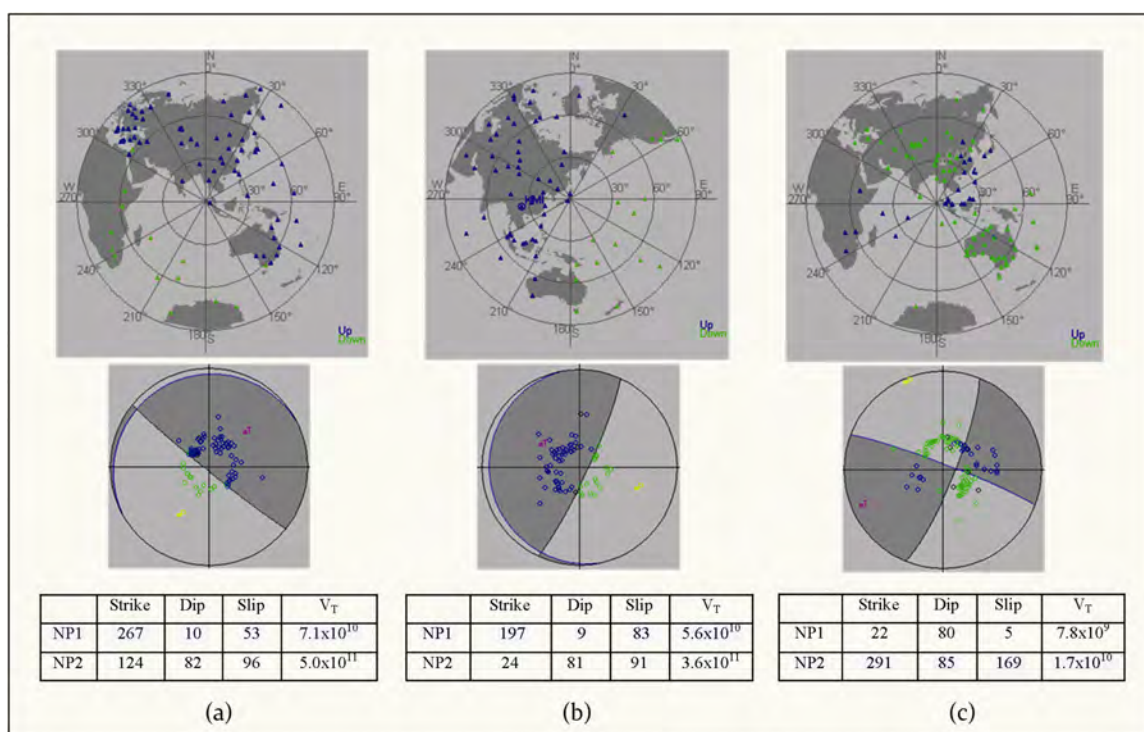


Fig. 11: Geographical distribution of first motion polarity (top row), focal mechanism beach ball diagram (middle row) and fault plane parameters along with V_T corresponding to both the nodal planes (NP1 and NP2) (bottom row) of a) Sumatra Earthquake on 26th December 2004 of Magnitude 9.1 b) Japan Earthquake on 11th March 2011 of Magnitude 9.0 and c) Indian Ocean Earthquake on 11th April 2012 of Magnitude 8.6. Both a) and b) are of thrust type fault and had produced ocean-wide tsunami. On the other hand c) is of strike-slip type fault and had produced local/regional tsunami.

This data is de-tided using prediction error filter to remove the natural tide from the data and monitored continuously for detection of tsunami waves.

Results and Discussion

The software has been tested with the following earthquakes: a) Sumatra Earthquake on 26 December 2004 of Magnitude 9.1, b) Japan Earthquake on 11th March 2011 of Magnitude 9.0 and c) Indian Ocean Earthquake on 11th April 2012 of Magnitude 8.6. Geographical distribution of first motion of P wave at global seismic stations and focal mechanism beach ball diagram obtained using SAGE module are shown in Fig. 11 (blue mark represents first motion up wards and green downward first motion). Out of these two focal plane parameters (blue and black lines in the beach ball diagram), the primary focal plane is determined by the known tectonic setting of that region and it

is passed on to the tsunami estimation module. In case where tectonic setting is not known beforehand, tsunami estimation is done for both the focal plane solutions.

Conclusion

Using near real time global seismic data, a quick and easy to use method of estimating earthquake source parameters including location, magnitude and its focal mechanism has been developed and implemented into an in-house software for prompt identification of tsunamigenic earthquakes from Indian Ocean region. Although accuracy of the focal plane parameters depends on the availability of seismic stations with good azimuthal coverage, but it is sufficient to distinguish between a thrust fault event and a strike slip event. Estimation of the volume of water displaced from the earthquake fault parameters and magnitude has been used to take a

decision about the type of tsunami it will generate. This technique has been tested with some tsunamigenic and non-tsunamigenic earthquakes which have occurred in the past. Further, tsunami generation is confirmed with near real time tide gauge stations available over the internet. The performance of the system is limited by the availability of near real time seismic and tide gauge data over the internet. The problem may be overcome by waveform modeling techniques so that fault plane parameters could be obtained using fewer stations' data.

Acknowledgement

The seismic data obtained for this software is downloaded from IRIS [2]. Figure 1 - 6 have been taken from site [3]. Authors are grateful to Dr. F. Roy, former Head, Seismology Division for his guidance to bring this work to a logical conclusion. Authors would also like to thank Shri C. K. Pithawa, Director E&IG and AMG and Dr R. K. Singh, Associate Director, RDDG for their kind support.

References

1. Roy Falguni and Nair G. J., "A Real Time Seismic Monitoring and Tsunami Alert System", *International workshop on external flooding hazards at NPP sites, Organized by AERB, NPCIL and IAEA*, 29 August - 02 September, 2005, Kalpakkam, India.
2. IRIS : <http://www.iris.edu>
3. S. Stein and M. Wysession, *An Introduction to Seismology, Earthquakes, and Earth Structure*, Blackwell Publishing, 2003 , <http://epsc.wustl.edu/seismology/book/>
4. Okal E. A. and Talandier J., "Mm- A Variable-Period Mantle Magnitude", *Journal of Geophysical Research*, 94(B4), 1989.
5. Talandier J. and Okal E. A., "An Algorithm for Automated Tsunami Warning in French Polynesia Based on Mantle Magnitudes", *Bulletin of the Seismological Society of America*, 79(4), 1989.
6. Kanamori H, "Mechanism of Tsunami Earthquakes", *Physics Earth Planet. Interiors*, 6, 1972.
7. Hanks T.C. and Kanamori H. , "A Moment Magnitude Scale", *Journal of Geophysical Research*, 84(B5), 1979.
8. International Tsunami Information Center: <http://itic.ioc-unesco.org>.
9. ETOPO Global Relief Model: <http://www.ngdc.noaa.gov/mgg/global/global.html>

Phase Transformation and Deformation Studies in Zr Based Alloys

K.V. Mani Krishna, D. Srivastava and G.K. Dey

Materials Science Division

Abstract

A brief account of microstructural and textural changes taking place during the processing of the Zirconium alloys and their role in the hydriding behavior is presented. The linkage between the microstructural evolution and textural development is demonstrated in case of processing of nuclear reactor's structural components. A new methodology for the reconstruction of the high temperature phase microstructure, using which the significant variant selection taking place during the transformation of β -Zr into α -Zr is demonstrated. The role of microstructure on the hydride formation is discussed in terms of effect of grain/phase boundaries.

Introduction

The importance of Zr based structural components in the thermal nuclear reactors can not be overemphasized. Pressure tubes, clad tubes are but few examples of several crucial Zr based 'in-reactor' components in PHWR type of reactors. The service performance of these components largely depends on their as-fabricated microstructure and texture. In addition, hydride formation, irradiation creep and growth are some of the important life limiting phenomena which are directly influenced by the component's microstructural and textural conditions. Hence it is important to understand (a) the evolution of the microstructure and texture during the fabrication (b) the role of the microstructure on the phenomena like hydride formation etc [1]. Such understanding helps tailoring the microstructures to mitigate the ill effects of the hydride formation. Understanding of the microstructural evolution as a function of process parameters, on the other hand, helps in optimizing the fabrication flow sheet to obtain the desired microstructures for enhanced component performance.

Present paper presents an overview of microstructural and textural evolution studies in various Zr based alloys and the microtextural aspects of various phase transformations in them.

Application of this knowledge for the design and implementation of new fabrication route for the production of pressure tube shall be described.

Deformation heterogeneity in Zr : Understanding through dislocation dynamics:

In view of its importance in microstructural and textural evolution, orientation sensitive deformation heterogeneity in Zr has been studied in detail. Clear evidences of temperature and orientation dependent heterogeneous plastic deformation were observed in zirconium when subjected to plane strain compression. Heterogeneities were in terms of grain fragmentation and apparent strain partitioning. Near basal grains showed least fragmentation, in-grain misorientation developments and changes in aspect ratio during room temperature rolling. This was diminished significantly during warm (500 and 700 K) rolling, see Fig 1(a). To address these experimental observations, dislocation dynamics (DD) simulations were carried out. These simulations, incorporating temperature dependent threshold criterion for the activation of slip systems, were successful in capturing the experimental observations, Fig. 1(b). DD simulations also brought out a novel mode of

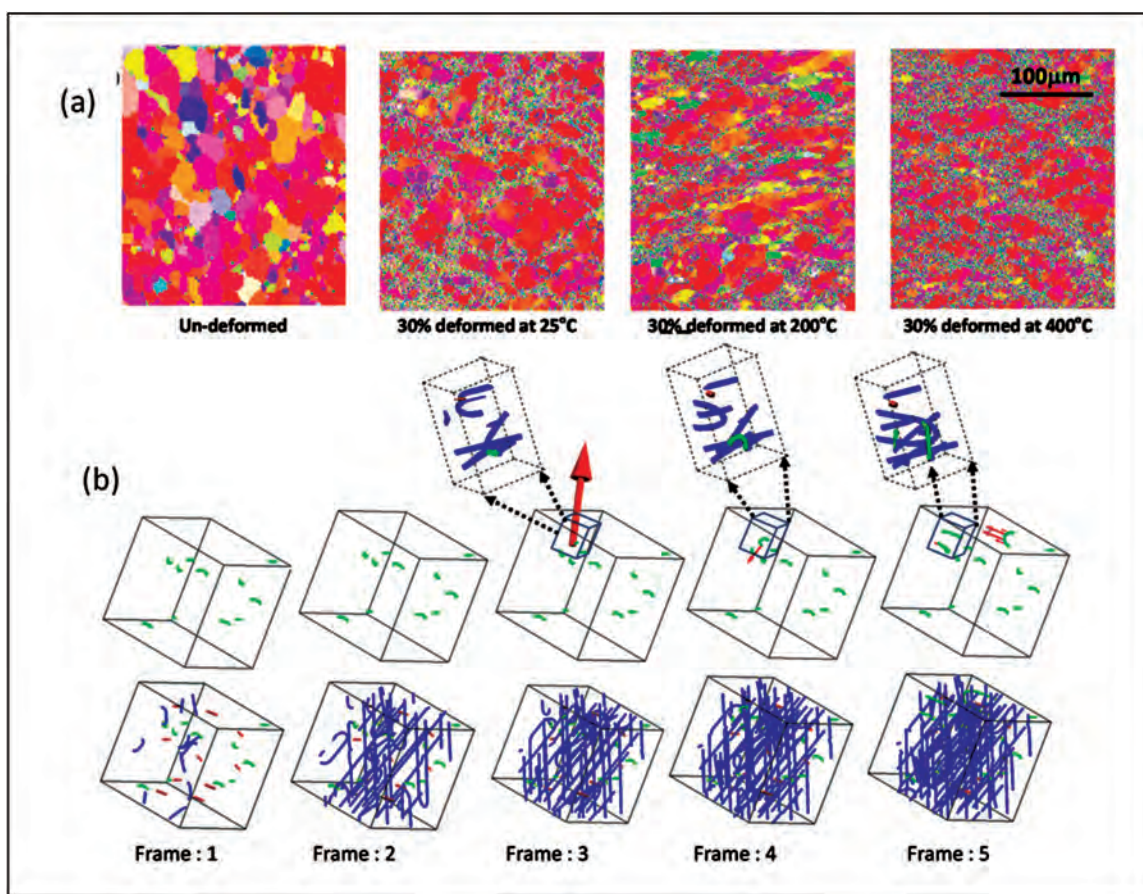


Fig.1: (a) Inverse pole figure (IPF) maps of Zircaloy 2 at different working temperatures. It is evident that some grains which are shown in 'red' having basal orientation are non-deformed at 30% of reduction at room temperature. The same grains, however, at higher temperature can be seen to elongate. (b) Snap shots of DD simulations showing the activation of the secondary dislocation sources. For these simulations, the orientation of the crystal with respect to the applied stress is such that prismatic dislocations (green ones in the figure) did not have any resolved forces along them. However, they did get activated once the other moving dislocations (pyramidal dislocations shown in blue) approach them closely due to interaction forces. The arrows indicate the resolved (along local burgers vectors) forces acting on the prismatic dislocations.

activation of dormant slip systems through interaction of active dislocations. Dormant slip systems, slip systems where the applied stress was below critical resolved shear stress, were activated due to interactions with active primary dislocations. This mechanism was shown to activate dormant dislocations in basal orientations, thus contributing to reduction in deformation heterogeneities during warm rolling. The proposed mechanism also has the potential to alter orientation sensitive plastic deformation in hexagonal metallic materials.

Reconstruction of high temperature β phase

As shown in the previous section one of the important steps of the component fabrication is the β -quenching step which results in texture randomization. However, the degree of texture randomization and the resulting microstructure subsequent to quenching are functions of nature of the phase transformation and microstructure of high temperature phase. Hence, knowledge of microstructure of high temperature phase and nature

of transformation in terms of variant selection can be helpful in optimizing the quenching parameters. In this context we had developed an algorithm to reconstruct the microstructure of the high temperature phase using the micro-texture data (EBSD data) of the room temperature phase [3].

The principle of reconstruction is based on the fact that in case of Burger's orientation relationship (OR)¹, each α grain (product) can have 6 possible β (parent) variants. Hence by considering at least three grains which have formed from same parent β grain, it is possible to deduce the orientation of the parent grain and thus reconstruct the parent microstructure. The algorithm employs a unique orientation based weightage factor, when there are more than three product grains resulting from same parent grain, to arrive at optimal solution for the parent phase orientation.

Based on the above algorithm, we reconstructed various transformed microstructures in case of Zircaloy-4 samples which have undergone a wide range of transformations ranging from diffusional to martensitic. An example of such reconstructed microstructure is presented in the Fig. 3, which also shows the identification of the product variants based on the just mentioned algorithm. It is clear that

there is considerable degree of variant selection (see Fig. 2d).

It is to be noted that the β to α phase transformation in case of Zr based alloys follows Burger's orientation which is crystallographically represented as $\{0\ 0\ 0\ 1\}_\alpha // \{1\ 1\ 0\}_\beta$ and $\langle 1\ 1\ \bar{2}\ 0 \rangle_\alpha // \langle 1\ 1\ 1 \rangle_\beta$

Some of the important advantages of this algorithm in comparison to other existing ones are its (a) less sensitivity to measurement errors in orientation measurement (b) practical elimination of spurious unification of the grains belonging to different parent grains (c) independence of calculated solution from user defined angular tolerance (δ_{max}).

Thus we are able to reconstruct the high temperature microstructure, and correlate the observed textural developments by identifying the variant selection taking place during the phase transformation using the just mentioned algorithm. This capability is expected to be of immense help in optimizing the β quenching process and gaining further insight into the mechanism of β to α phase transformation.

Role of grain/phase boundaries in hydride formation

Hydride formation is known to be one of the life limiting factors in case of Zr based structural components used in thermal nuclear reactors.

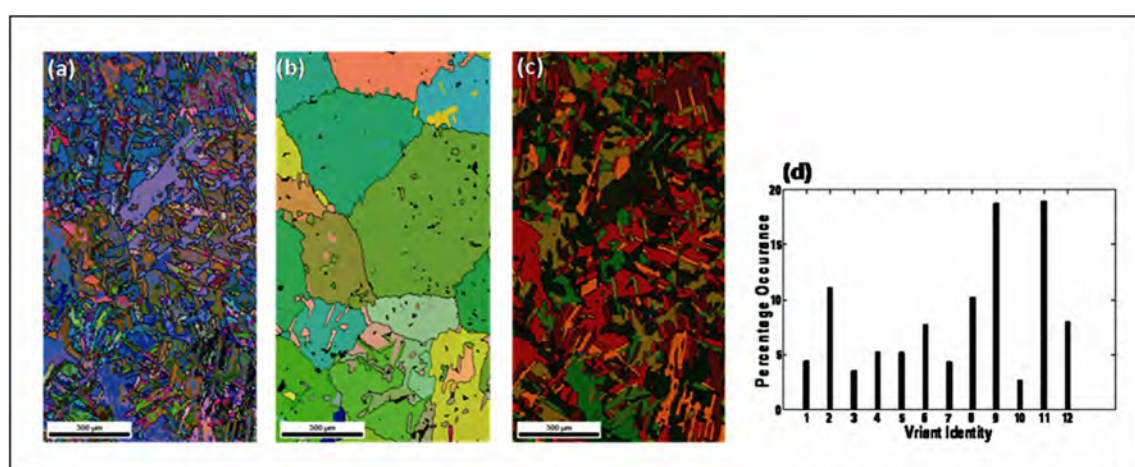


Fig.2: (a) EBSD microstructure of β quenched microstructure of Zircaloy-4 (b) The reconstructed map of parent phase (β) (c) Microstructure of product phase with each product grain colored according to its variant identity (d) Frequency distribution of product variants.

Understanding the mechanism of hydride formation can help tailor the suitable microstructures for better hydride mitigation in these alloy components. However, very little information was available on the role of nature of the grain boundaries and interfaces in controlling the hydride formation [4, 5]. In the present article we report, substantial improvement in understanding of the role of grain/phase boundaries with explicit use of local orientation measurements through EBSD technique.

Fig. 3 depicts the hydride microstructures in case of single phase (Zircaloy-2) and two phase (Zr-2.5Nb) Zr alloys. It is quite evident that majority of hydrides were along α/α boundaries in case of Zircaloy-2 and α/β interfaces in case of Zr-2.5Nb alloy. A detailed analysis of the microtexture data on these hydride samples revealed following important facts on the preference of hydrides for particular interfaces.

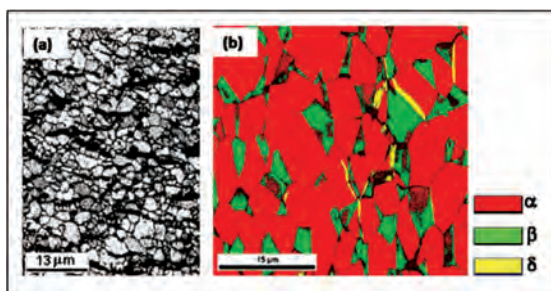


Fig. 3: Hydride distribution in Zirconium based alloys (a) Zircaloy-2 (b) Zr-2.5%Nb alloy. It is clear that in both the cases the hydride phase is along the interfaces of the grains only

- In case of single phase alloy, (Zircaloy-2), formation of hydrides was preferred on certain grain boundaries. Those boundaries which are characterized by low coincident site lattice (CSL) values, in general, were resistant to hydride formation.
- Hydrides in the two phase Zr-2.5%Nb alloy in a completely recrystallized condition have formed primarily along α/β interfaces, with only a minor fraction of hydrides being along α/α grain boundaries.

- Majority of the hydrides were along those α/β interfaces which had a misorientation corresponding to burger's OR. However, not all the α/β interface which are related by the burger's OR are having the hydrides along them. Selection of α/β interfaces as the favorable nucleation sites by the hydrides was attributed to high hydrogen partitioning between the α and β phases on account of the large differences in solid solubilities of hydrogen in α and β phases. This makes α/β interfaces to be the nearest available heterogeneous nucleation sites for most of the hydrogen atoms.

Development of new fabrication route for Zr-2.5Nb pressure tube

It is well known that Indian PHWRs employ Zr-2.5%Nb based pressure tubes. These tubes are being so far manufactured in NFC, Hyderabad, using a double cold pilgering and double hot extrusion process. In the context of upcoming reactors where higher design life of these tubes are being sought with improved creep resistance, an exercise to optimize the existing processing route was initiated with the collaboration of NFC, Hyderabad. Different fabrication trails involving the variation in three important stages of Zr-2.5%Nb pressure tube were undertaken. The variations were with respect to mode of breaking the cast structure of the ingot (forging vs. extrusion), ratio of hot extrusion and number of stages of subsequent cold work to produce the finished tube. It was observed that forging process resulted in superior performance in breaking the cast structure. Higher extrusion ratios resulted in more favorable texture and microstructure. Continuity of the beta phase in the final microstructure was observed to be more in case of route involving single cold work subsequent to hot extrusion. The final microstructure generated using the modified route had more desirable aspect ratio of alpha grains and relatively more continuous beta phase and is expected to have better creep resistance. It was also shown that the end to end variation in properties of the tube generated by the new route

is superior to that of the conventional route. The modified route has actually been accepted and inducted for the production of the pressure tubes for the upcoming reactor.

Acknowledgements

Significant part of the above research was in active collaboration with Prof. I Samajdar, IIT Bombay and Shri. N. Saibaba, NFC, Hyderabad. We gratefully acknowledge their contributions to this research.

References

1. D O Northwood, U. Kosasih, *Int Met Rev* (1983) 28- 92
2. V Randle V, O Engler, *Introduction to Texture Analysis Microtexture and Orientation Mapping*, ISBN 90-5699-224-4, Taylor and Francis Limited, 11 New Fetter Lane, London, UK, 2003.
3. K V Mani Krishna, P Tripathi, V D Hiwarkar, P Pant, I Samajdar, D Srivastava, G K Dey, *Scripta Materilia*, 62, (2010) 391-394.
4. K V Mani Krishna, D Srivastava, G K Dey, V Hiwarkar, I Samajdar, S Banerjee, *J Nucl Mater.* 414 (2011) 270-275.
5. K V Mani Krishna, A Sain, I Samajdar, G K Dey, D Srivastava, S Neogy, R Tewari and S Banerjee, *Acta Materilia* 54(2006) 4665-4675.

Assessment of Higher Order Shear and Normal Deformations Theories for Stress Analysis and Free Vibration of Functionally Graded Plates

D.K. Jha and K. Srinivas

Civil Engineering Division

and

Tarun Kant

Department of Civil Engineering,

Indian Institute of Technology Bombay, Mumbai

and

R.K. Singh

Reactor Safety Division

Abstract

Stress analysis and free vibration of functionally graded (FG) elastic, rectangular, and simply (diaphragm) supported plates are presented based on higher order shear/shear-normal deformations theories (HOSTs/HOSNTs). The theoretical models are based on Taylor's series expansion of the in-plane and transverse displacements in the thickness coordinate defining the plate deformations. The material properties of FG plates are assumed in this case to be varying through the thickness of the plate in a continuous manner according to the volume fraction of constituents which is mathematically modelled as exponential and power law functions. The governing equations for the FG plates are derived on the basis of HOSTs/HOSNTs assuming varying material properties. Analytical solutions are obtained by employing the Navier solution technique. Accuracy of the analytical solutions obtained employing Navier solution technique using present models has been compared with exact three dimensional (3D) elasticity solutions.

Keywords: Functionally graded materials; higher order, analytical solutions; stress analysis, natural frequency; material grading index.

Introduction

Functionally graded materials (FGMs) are recent development in the family of engineering composites made of two or more constituent phases with continuous and smoothly varying composition [Koizumi¹]. This has been possible through research and development in the area of mechanics of FGMs for the present day modern technologies of special nuclear components, spacecraft structural members, ceramics and composites etc. To improve the properties of thermal-barrier systems, FGMs consisting of metallic and ceramic components are preferred because cracking or de-lamination, which are often observed in conventional multi-layer

systems are avoided due to the smooth transition between the properties of the components. With the increase in application of FGMs in various fields of science and technology, new methodologies need to be developed to characterize FGMs and also designing structural components, viz., beams, plates and shells made of it. In view of its engineering application to create the divertor plate (also called, the first wall) of the International Thermonuclear Experimental Reactor (ITER) made of a graded layer bonded between a homogeneous substrate and a homogeneous coating, a two-dimensional (2D) model for the analysis of functionally graded (FG)

plate with reasonably high accuracy and computational efforts is rationalized.

Literature Review

Three-dimensional (3D) analytical solutions are very useful since they provide benchmark results to assess the accuracy of various 2D plate theories and finite element formulations, but their solution methods involve mathematical complexities and are very difficult and tedious to solve. The benchmark exact 3D elasticity solutions of simply supported laminated plates available in the literature [Refs. 2–5] have proved to be very useful in assessing two-dimensional (2D) plate theories by various researchers [Refs. 6–9]. There are many studies available in the literature as well on the analysis of isotropic, orthotropic and laminated composite plates, but these investigations are valid for laminated plates and shells, where the material properties are piecewise constant, but not applicable for finding solutions of plate problems with continuous in-homogeneity of material properties such as FGMs. Due to the special properties exhibited by the FGMs, such as high degree of anisotropy, higher load carrying capacity due to membrane-bending coupling for preferential structural performance, the method of analysis based on Classical Plate Theory (CPT) which neglects the effect of out-of-plane (transverse) stresses/strains become inadequate. First Order Shear Deformation Theory (FOST) assumes constant states of transverse shear stresses and requires the use of shear correction coefficients suggested by Mindlin (1951) for homogeneous isotropic plates in order to match the response predicted by this two-dimensional (2D) theory with that of three-dimensional (3D) elasticity theory and to simplify the shear stresses/strains through the plate thickness in an approximate manner, which at times may become unrealistic. Next in the line of the plate theories are the higher-order shear deformation plate theories which consider the warping of the cross-sections and satisfy the zero transverse shear stress condition of the upper and lower fibers of the cross-section. In the literature,

various higher-order shear deformation theories, viz. Second order shear deformation theory (SSDT), Third order shear deformation theory (TSDT) which satisfies the above-mentioned conditions are proposed by several researchers.

Suresh and Mortensen¹⁰ provided an excellent introduction to the fundamentals of FGMs. Since then, many publications are reported in the literature on the use of various two-dimensional (2D) theories for the thermo-elastic and vibration analyses of FG plates during the last few years. Both analytical and finite element methods are used for the analysis. Praveen and Reddy¹¹ reported the response of FG ceramic metal plates using a plate finite element formulation. Main and Spencer¹² constituted a class of exact 3D solutions for FG plates with traction-free surfaces. Vel and Batra¹³ presented the 3D exact solutions for the free and forced vibrations of simply supported FG rectangular plates by assuming the suitable displacement functions that identically satisfy boundary conditions. These displacement functions are used to reduce equations governing steady state vibrations of a plate to a set of coupled ordinary differential equations, which are then solved by employing the power series method. The exact solution is valid for thick and thin plates, and for arbitrary variation of material properties in the thickness direction. Carrera et al.¹⁴ studied the effects of stretching of thickness in FG plates and shells deriving the advanced theories for bending analysis adopting Reissner's mixed variational approach. Recently, Wen et al.¹⁵ have presented the 3D analysis of isotropic and orthotropic FG plates with simply supported edges under static and dynamic loads. The governing equations of the 3D elastic problem for the FG plates were formulated based on the state-space approach in the Laplace transform domain, transforming it to a one dimensional problem, and solved using the radial basis functions (RBF) method. For a complete reference on the recent research studies on the static, vibration and stability analyses of FG plates, the reader may refer the critical review on the subject matter by Jha et al.¹⁶. In most

of the 2D theories developed to predict the global responses of FG plates till date, only transverse shear deformations have been considered, and very few theories consider the effect of both transverse shear and transverse normal deformations. Very limited studies are reported in the literature on the evaluation of the various 2D higher order theories and about their range of application and the accuracy in predicting the global responses.

Theoretical Formulation

Owing to the above limitations, analytical formulations are developed using a set of displacement based higher order shear/shear-normal deformation theories (HOSTs/HOSNTs) for the stress analysis and free vibration of FG elastic, rectangular, and simply (diaphragm) supported plates. The theoretical models are based on Taylor’s series expansion of the in-plane and transverse displacements in thickness coordinate defining the plate deformations. Some of these models reformulated by Jha et al.¹⁷⁻¹⁸ for FG plates listed in Table 1 account for the effects of transverse shear and normal deformations and nonlinear variation of in-plane displacements. The material properties of FG plates are considered in this case to be varying through thickness of plate in a continuous manner. Poisson’s ratio is assumed to be constant, but their Young’s moduli and material density vary continuously in thickness direction according to the volume fraction of constituents which is mathematically modelled as exponential and power law functions, represented as:

$$\left. \begin{aligned} P(z) &= P_t \exp\left(-\lambda \left(1 - \frac{2z}{h}\right)\right), \text{ where, } \lambda = \frac{1}{2} \ln\left(\frac{P_t}{P_b}\right) \\ P(z) &= (P_t - P_b) \left(\frac{z}{h} + \frac{1}{2}\right)^k + P_b \end{aligned} \right\} (1)$$

Here P(z) denotes a typical material property, viz., Young’s modulus of elasticity (E), material density (\bar{n}), etc. of the structures made of FGM. h represents the total thickness of structure. P_t and P_b are the material properties at the top-most ($z = +h/2$) and bottom-most ($z = -h/2$) surfaces. λ in the

exponential model and k in the power model are the material grading indexes respectively.

The governing equations for the FG plates are derived on the basis of HOSTs/HOSNTs assuming varying material properties across thickness of plate. The equations of equilibrium are derived using Principle of Minimum Potential Energy (PMPE) and the equations of motion by Hamilton’s principle. Numerical solutions are obtained in closed-form using Navier’s solution technique. The membrane-flexure coupling phenomenon exhibited by a FG plate necessitates the use of a displacement field containing both, membrane as well as flexural deformation terms which contribute to the overall response of the plate. The displacements u, v and w of a general point (x, y, z) in the plate domain shown in Fig. 1 in x, y and z directions, respectively are given by:

$$\left. \begin{aligned} u(x,y,z) &= u_o(x,y) + z\theta_x(x,y) + z^2 u_o^*(x,y) + z^3 \theta_x^*(x,y) \\ v(x,y,z) &= v_o(x,y) + z\theta_y(x,y) + z^2 v_o^*(x,y) + z^3 \theta_y^*(x,y) \\ w(x,y,z) &= w_o(x,y) + \xi_1 z \theta_z(x,y) + \xi_2 z^2 w_o^*(x,y) + \xi_3 z^3 \theta_z^*(x,y) \end{aligned} \right\} (2)$$

Here, the parameters u_o, v_o are the in-plane tangential displacements and w_o is the transverse displacement of a point (x, y) on the plate’s middle surface. θ_x, θ_y are rotations of the normals to the plate’s middle surface ($z=0$) about y and x axes respectively.

$u_o^*, v_o^*, w_o^*, \theta_x^*, \theta_y^*, \theta_z^*$ and θ_z are the higher order terms in the Taylor’s series expansion and represent

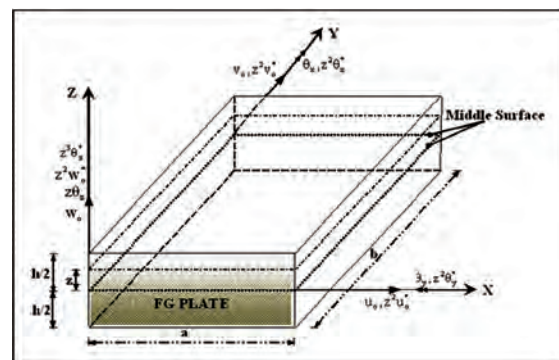


Fig. 1: Geometry of FG plate with positive set of reference axes and its displacement components (For “HOSNT12” model)

Table 1: List of displacement models based on higher order refined theories

Model	Theory	DOFs	Designation	Displacement field	Transverse shear deformations (γ_{xz} and γ_{yz})	Transverse normal deformation (ϵ_z)
1	HOSNT	12	HOSNT12	As defined in Eqn. (2) with $\xi_1 = \xi_2 = \xi_3 = 1$	Cubic	Parabolic
2	HOSNT	11	HOSNT11	As defined in Eqn. (2) with $\xi_1 = \xi_2 = 1; \xi_3 = 0$	Parabolic	Linear
3	HOSNT	11	HOSNT11M	As defined in Eqn. (2) with $\xi_1 = \xi_3 = 1; \xi_2 = 0$	Cubic	Parabolic
4	HOSNT	10	HOSNT10B	As defined in Eqn. (2) with $\xi_1 = \xi_3 = 0; \xi_2 = 1$	Parabolic	Linear
5	HOSNT	10	HOSNT10M	As defined in Eqn. (2) with $\xi_1 = 1; \xi_2 = \xi_3 = 0$	Parabolic	Constant
6	HOST	9	HOST9	As defined in Eqn. (2) with $\xi_1 = \xi_2 = \xi_3 = 0$	Parabolic	Not considered

the higher order transverse cross sectional deformation modes.

In addition to the above mentioned higher order models, the FOST¹⁹ and CPT²⁰ models are also considered for the analyses of FG plates for the sake of comparison.

Numerical Studies

A simply (diaphragm) supported rectangular/square plate is considered throughout as a test problem. Sinusoidal and uniform transverse loadings are considered for the stress analysis of FG Plates with various geometrical configurations and material

grading indexes. A set of computer programs based on the present models is developed in MATLAB7.0 to solve the boundary value problem for the stress analysis and eigenvalue problem for the free vibration. The numerical results for the stress analysis of FG plates are presented for in-plane and transverse displacements, in-plane normal and shear stresses and transverse shear stresses. Further, the natural frequencies of FG plates using various higher order models are also presented. The accuracy of solutions obtained from different models is established by comparing the results with the 3D exact elasticity solutions and the solutions obtained by various other models in literature.

Stress analysis of FG Plates

A sinusoidally loaded, simply (diaphragm) supported, FG square plate of side, $a=1\text{m}$ and thicknesses-to-width ratio, $h/a=0.1$ is considered as in Ref.15. The elastic moduli are $E_t=70\text{ GPa}$, $E_b=151\text{ GPa}$, and the Poisson’s ratio is $\nu=0.3$. Here E_t and E_b indicate Young’s moduli on the top (i.e., $z=+h/2$) and bottom (i.e., $z=-h/2$) surfaces of the FG plate, respectively. The normalized static load is assumed as $q(x, y)=-q_0 \sin(\pi x/a)\sin(\pi y/a)$, where, $q_0=10^{-3}C^{0_{33}}$, in which, $C^{0_{33}}=E_b(1-\nu)/[(1+\nu)(1-2\nu)]$. The variation of material properties in plate’s thickness direction is considered to follow an exponential law, i.e., $C^{z_{ij}}=C^{0_{ij}} e^{\lambda(z+h/2)}$, where $C^{0_{ij}}$ indicates material coefficients on the bottom surfaces, and the material gradation coefficient, $\lambda(=\ln(E_t/E_b))$. The analytical solutions for deflections and stresses of the FG plate are available at point $(a/4, a/4, -h/4)$ by Wen et al.¹⁵ using RBF interpolation. Exact elasticity solutions of the same problem are also available in Zhang and Zhong²¹. The non-dimensional displacements and stresses parameters are evaluated at the same point $(a/4, a/4, -h/4)$ using various models considered in the present study for validation.

The solutions obtained using models HOSNT12 and HOSNT11 are in close agreement with 3D elasticity solutions of the same problem by Zhang and Zhong²¹. It is found here that HOSNT12 computes the most accurate results with 0.006% errors in the in-plane displacements and 0.003% error in transverse deflection which are best among all other analytical solutions including the RBF analytical solutions¹⁵ with highest number of collocation points. HOST9 computes the displacements with a maximum error of 1.045% for a moderately thick FG plate ($h/a=0.1$). HOSNT11M and HOSNT10M models fall short here to predict the static behaviour of FG plates with a significant error of about 18% in displacements. The HOSNT12 model is the most accurate with the errors of -0.502% and -0.004% in σ_x and τ_{xy} . The error in transverse shear stresses is of identical order for all higher order formulations.

The variation of some of these non-dimensional displacements and stresses parameters at the point $(x=a/4, y=a/4)$ along the thickness of FG plates ($h/a=0.25$) are plotted in Figs. 2-4 using the present formulations. Here, it is worth noting that, neutral surface of the FG plate does not coincide with the middle surface ($z=0$) of the plate, and it is found to be at $z=-0.055h$. This shift of the neutral surface is towards the stiffer material side. It can be very clearly pointed out from the presented results, that the higher order transverse normal deformation terms in choosing the displacement field cannot be neglected in the formulation for the thick FG plates, especially when the thicknesses-to-width ratio (h/a) equals or more than 0.2. This highly accurate 2D formulation can be used to capture the behaviour of transversely loaded FG plates more closely, especially for thicker plates ($h/a \geq 0.1$), and it is totally justified when the thicknesses-to-width ratio (h/a) exceeds 0.2. Using this higher order displacement formulation, the transverse loads can be considered acting at any surface of the plate.

Free vibration of FG Plates

Using various displacement models considered in the present study, the non-dimensional fundamental natural frequency are computed for FG plates comprised of aluminum (Al) and zirconia (ZrO_2). The comparisons of present results with the available TSDT solutions in Ferreira et al. 22 are presented in Table 2. The different in-plane harmonics for FG

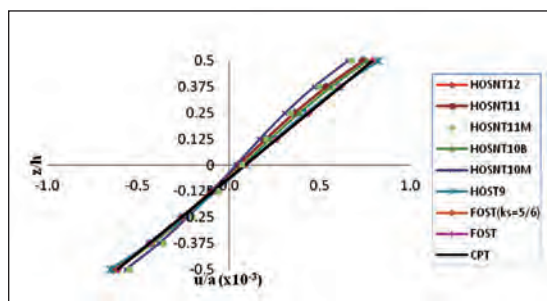


Fig. 2: Through thickness variations of in-plane displacement of simply (diaphragm) supported FG square plates ($h/a=0.25$) under sinusoidal load

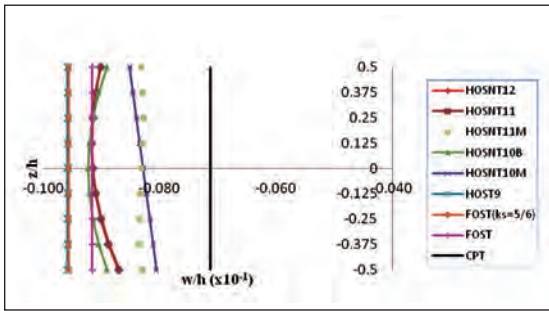


Fig. 3: Through thickness variations of transverse displacement of simply (diaphragm) supported FG square plates ($h/a=0.25$) under sinusoidal load

plates are computed using the present higher order theories and compared with SSDT solutions by Shahrjerdi et al. 23 in Table 3.

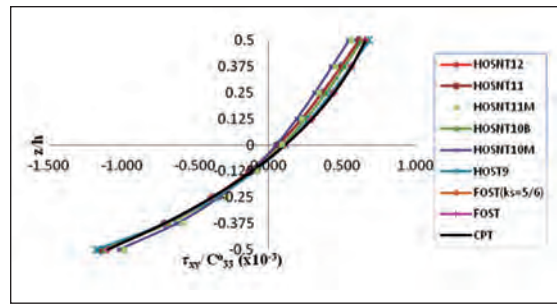


Fig. 4: Through thickness variations of in-plane shear stress of simply (diaphragm) supported FG square plates ($h/a=0.25$) under sinusoidal load

Concluding Remarks

From the extensive set of results obtained in the present study, it has been observed that the higher order theories which do not satisfy the zero

Table 2: Non-dimensional fundamental natural frequency of FG square plates

Theory	Non-dimensional fundamental natural frequency $\hat{\omega}_{mn} (m = n = 1) = \omega_{mn} (h) \sqrt{\frac{\rho_m}{E_m}}$					
	Material Properties: Metal (Al): $E_m = 70 \text{ GPa}, \rho_m = 2702 \text{ Kg/m}^3, \nu = 0.30$ Ceramic (ZrO2): $E_c = 200 \text{ GPa}, \rho_c = 5700 \text{ Kg/m}^3, \nu = 0.30$					
	$h/a=0.05$	$h/a=0.1$	$h/a=0.2$			
	k=1	k=1	k=1	k=2	k=3	k=5
Exact ^a	0.0153	0.0596	0.2192	0.2197	0.2211	0.2225
TSDT ^b	0.0147	0.0592	0.2188	0.2188	0.2202	0.2215
HOSNT12	0.0153	0.0598	0.2219	0.2220	0.2227	0.2237
HOSNT11	0.0153	0.0598	0.2219	0.2220	0.2227	0.2237
HOSNT10B	0.0154	0.0599	0.2239	0.2239	0.2244	0.2250
HOSNT11M	0.0167	0.0655	0.2402	0.2403	0.2406	0.2413
HOSNT10M	0.0167	0.0655	0.2402	0.2403	0.2406	0.2413
HOST9	0.0153	0.0599	0.2211	0.2212	0.2218	0.2227
FOST ($k_s=5/6$)	0.0154	0.0601	0.2217	0.2219	0.2231	0.2246
FOST	0.0156	0.0610	0.2248	0.2250	0.2264	0.2280
CPT	0.0162	0.0656	0.2500	0.2502	0.2529	0.2561

^a Taken from Vel and Batra¹³

^b Taken from Ferreira et al.²²

Table 3: Natural frequencies of rectangular FG plates ($b/a=2, h/a=0.1$)

Mode	mxn	Non-dimensional natural frequencies,, $\tilde{\omega}_{mn} = \omega_{mn} \left(\frac{a^2}{h}\right) \sqrt{\rho_c/E_c}$							
		Material Properties: Metal (Al): $E_m=68.9$ Gpa, $\nu=0.33, \rho_m=2700$ kg/m ³ Ceramic (ZrO ₂): $E_c=211$ Gpa, $\nu=0.33, \rho_c=4500$ kg/m ³							
		k=0		k=0.5		k=1		k=2	
		SSDT ^c	HOSNT12	SSDT ^c	HOSNT12	SSDT ^c	HOSNT12	SSDT ^c	HOSNT12
1.	1x1	3.6983	3.6911	3.3713	3.3664	3.2225	3.2179	3.1354	3.1291
2.	1x2	5.8498	5.8323	5.3359	5.3238	5.1002	5.0886	4.9594	4.9434
3.	2x1	12.0345	11.965	10.9940	10.946	10.5062	10.461	10.1985	10.137
4.	2x2	14.0144	13.921	12.8103	12.745	12.2421	12.180	11.8784	11.794
5.	2x3	17.2325	17.096	15.7660	15.668	15.0670	14.973	14.6092	14.481
6.	3x2	26.3462	26.051	24.1494	23.941	23.0749	22.876	22.3273	22.059
7.	3x3	29.2257	28.871	26.8100	26.554	25.6184	25.372	24.7781	24.446

^cTaken from Shahrjerdi et al.²³

transverse shear stress condition at the top and bottom bounding planes of the FG plates give the most accurate values of displacements, stresses, and natural frequencies as compared to other theories in the case of thick plates. On the basis of the analysis carried out and the numerical results obtained the following conclusions are drawn:

1. It is evident from the numerical solutions presented for FG plates that its neutral surface does not coincide with the middle surface as in the case of isotropic and orthotropic plates. The shift of neutral surface is always towards the stiffer material zone. The location of the neutral surface of FG plates depends upon its material gradation coefficient/index in the spatial direction. The shift of the neutral surface from the middle surface also depends upon thickness of plate. Thicker the plates, lesser will be the shift of neutral surface. The location of neutral surface of FG plates does not depend upon the aspect ratio of the plate and the magnitude and kind of external loads applied.
2. The higher order models HOSNT12 and HOSNT11 evaluate the bending responses of thin

and thick FG plates very close to 3D elasticity exact solutions. It brings out the fact that both transverse shear and normal deformations has to be taken in to account in the analysis of thick plates which undergoes cross sectional warping. For flexure dominated problems of FG plates, the contribution/ effect of higher order membrane term (θ_z^*) in transverse displacement field is not of much significance.

3. Although the presented formulation for FG plates using HOSNT12/HOSNT11 involves large computations compared to FOST and CPT, but the obtained numerical results are very accurate when compared to the 3D elasticity solutions. The benefit of this approach is that a 2D theory is able to predict solutions very close to 3D elasticity solutions.

Acknowledgments

Authors wish to thank authorities of Bhabha Atomic Research Centre (BARC), Department of Atomic Energy, Mumbai, India and Indian Institute of Technology (IIT) Bombay, Mumbai, India for providing the help and support.

References

1. Koizumi, M. "FGM activities in Japan". *Composites Part B*, 28B, (1997): 1-4.
2. Pagano, N.J. "Exact solutions for composite laminates in cylindrical bending". *J. Composite Mater.*, 3, (1969): 398-411.
3. Pagano, N.J. "Exact solutions for rectangular bidirectional composite and sandwich plates". *J. Composite Mater.*, 4, (1970): 20-34.
4. Srinivas, S. and Rao, A.K. "Bending, vibration and buckling of simply supported thick orthotropic rectangular plates and laminates". *Int. J. Solids Struct.*, 6(11) (1970): 1463-1481.
5. Srinivas, S., Joga Rao, C.V. and Rao, A.K. "An exact analysis for vibration of simply supported homogeneous and laminated thick rectangular plates". *J. Sound Vib.*, 12(2), (1970): 187-99.
6. Pandya, B.N. and Kant, T. "Higher order shear deformable theories for flexural of sandwich plates: finite element evaluations". *Int. J. Solids Struct.* 24(12), (1988): 1267-1286.
7. Kant, T. and Manjunatha, B.S. "On accurate estimation of transverse stress in multilayer laminates. *Computers and Structures*, 50(3), (1994): 351-365.
8. Kant, T. and Swaminathan, K. "Analytical solutions for the static analysis of laminated composite and sandwich plates based on a higher-order refined theory". *Composite Structures*, 56, (2002): 329-344.
9. Reddy, J.N. *Mechanics of Laminated Composite Plates: Theory and Analysis*, CRC, New York, 1997.
10. Suresh, S. and Mortensen, A. *Fundamentals of Functionally Graded Materials*. 1st edition, IOM Communications: London, 1998.
11. Praveen, G.N. and Reddy, J.N. "Nonlinear transient thermoelastic analysis of functionally graded ceramic-metal plates". *Int. J. Solids Struct.* 35, (1998): 4457-4471.
12. Main, A.M. and Spencer, A.J.M. "Exact solutions for functionally graded and laminated elastic materials". *J. Mech. Phys. Solids*, 46(12), (1998): 2283-95.
13. Vel, S.S. and Batra, R.C. "Three-dimensional exact solution for the vibration of functionally graded rectangular plates". *Journal of Sound and Vibration*, 272, (2004): 703-730.
14. Carrera, E., Brischetto, S. and Robaldo, A. "Variable kinematic model for the analysis of functionally graded material plates". *AIAA J.*, 46, (2008): 194-203.
15. Wen, P.H., Sladek, J. and Sladek, V. "Three-dimensional analysis of functionally graded plates". *Int J Numer Meth Eng*, 87(10), (2011): 923-942.
16. Jha, D.K., Kant, T., and Singh, R.K. "A critical review of recent research on functionally graded plates". *Composite Structures*, 96, (2013): 833-849.
17. Jha, D.K., Kant, T. and Singh, R.K. "Stress analysis of transversely loaded functionally graded plates with a higher order shear and normal deformation theory". *ASCE Journal of Engineering Mechanics*, 139 (12), (2013): 1663-1680.
18. Jha, D.K., Kant, T., and Singh, R.K. "Free vibration response of functionally graded thick plates with shear and normal deformations effects". *Composite Structures*, 96, (2013): 799-823.
19. Whitney, J.M. and Pagano, N.J. "Shear deformation in heterogeneous anisotropic plates". *ASME Journal of Applied Mechanics*, 37(4), (1970): 1031-1036.
20. Timoshenko, S.P. and Woinowsky-Krieger, S. *Theory of Plates and Shells*, 2nd Edn., McGraw-Hill, Singapore, 1959.
21. Zhang, C. and Zhong, Z. "Three-dimensional analysis of a simply supported functionally graded plate based on Haar Wavelet method".

Acta Mechanica Solida Sinica, 28(3), (2007): 217-223.

22. Ferreira, A.J.M., Batra, R.C, Roque, C.M.C., Qian, L.F. and Jorge, R.M.N. "Natural frequencies of functionally graded plates by a meshless method". *Composite Structures*, 75, (2006): 593-600.
23. Shahrjerdi, A., Mustapha, F., Bayat, M., Sapuan, S.M., Zahari, R. and Shahzamanian, M.M. "Natural frequency of F.G. rectangular plate by shear deformation theory". *IOP Conf. Series: Materials Science and Engineering*, 17(1), (2011): 1-6.

The elusive neutrino

V.M. Datar
Nuclear Physics Division

Abstract

After briefly introducing the neutrino the observations that led to the discovery of neutrino oscillations are described. Various sources of neutrinos have been used to uncover facets of neutrinos including the more recent measurement of one of key neutrino parameters in a reactor based experiment at Daya Bay, China. The Indian effort to build an underground laboratory for rare processes is outlined. The flagship experiment to measure atmospheric muon neutrinos and antineutrinos, separately, will target the open problem of ordering of the 3 tiny neutrino masses. Together with other experiments worldwide this will help address CP violation in the neutrino sector. This could help us understand why there is a preponderance of matter over anti-matter in the universe we live in.

Introducing neutrinos

The neutrino is an elementary particle proposed by Wolfgang Pauli (Fig.1) in 1930 to explain the continuous energy spectrum of electrons in nuclear beta decay. The neutrino has no electric charge, a tiny mass a millionth of that of an electron and interacts weakly [1] with matter. The weak interaction [2] is responsible for the beta decay of nuclei such as ^{14}C (used in dating substances containing organic carbon) and ^{40}K (present at a level of about 100 parts per million in all naturally occurring potassium). Were it much stronger, for example, of the order of the electromagnetic (EM) interaction, the sun would have burnt itself out in a matter of days rather than billions of years. Among other consequences, this would have made impossible the evolution of life, as we understand it.

The neutrino is the second most abundant particle in the universe (~ 330 neutrinos/cm³), after the photon, the quantum of electromagnetic interactions. However because of its weak interaction and low energy (~ 170 μeV), the cosmic neutrinos, which are relics of the big bang explosion that resulted in our universe, remain undetected. In contrast the cosmic EM radiation is characteristic

of a blackbody at 2.7°K, peaks in the microwave region. Its measurement by space based radio telescopes have allowed us to infer the fluctuations in the very early stages of the universe leading to the present day large scale structure of the universe. In the Standard Model of particle physics, whose predictions have been extensively verified, the neutrino mass is expected to be zero. The three varieties of neutrinos belonging to the electron, muon and tau lepton families, also transform into one another, a phenomenon known as neutrino oscillations.

Because of their weak interaction with matter, unlike EM radiation, neutrinos can penetrate matter effortlessly. For example a neutrino, with an energy $\sim \text{MeV}$, has a probability of only 10^{-10} of interacting with matter were it to traverse the diameter of the earth. It is this property that has enabled scientists



Fig. 1: (Left to Right) W. Pauli, E. Fermi, C.L. Cowan and F. Reines

Box 1. Nuclear reactions powering the sun

The *pp* chain reactions, proposed by Hans Bethe (Nobel prize in Physics 1967) occur in the core of the sun where the temperature reaches 15,000,000 °K. The reactions are:

$$p+p \rightarrow d+e^++\nu_e$$

$$d+p \rightarrow {}^3\text{He}+\gamma$$

$${}^3\text{He}+{}^3\text{He} \rightarrow {}^4\text{He}+2p$$

$${}^3\text{He}+{}^4\text{He} \rightarrow {}^7\text{Be}+\gamma, {}^7\text{Be}+p \rightarrow {}^8\text{B}+\gamma$$

$${}^8\text{B} \rightarrow {}^8\text{Be} + \beta^++\nu_e, {}^8\text{Be} \rightarrow {}^4\text{He} + {}^4\text{He}$$

$4p \rightarrow {}^4\text{He} + 2\beta^- + 2\nu_e$ releasing ~ 24 MeV energy

to peer into the heart of the sun and confirm that the *p-p* fusion reaction chain (see Box 1) is responsible for its huge energy production. Violent explosions that could occur towards the end of a star’s life, called supernovae, can also be studied through neutrinos produced during the neutronization (where electrons and protons combine to form a neutron and a neutrino).

Historically, the theory for β -decay [3] was first formulated by Enrico Fermi, the famous Italian-American physicist (awarded the Nobel prize in Physics for work on slow neutron induced transmutation of nuclei in 1938). The theory was modeled on the theory of EM interactions. It also discussed the method for measuring the mass of the neutrino through a measurement of the shape of the beta spectrum near the end point. It was

Fermi who gave this new neutral particle a name viz. the little neutron or *neutrino*. The neutrino was first detected in a reactor experiment [4] by Cowan and Reines in 1956. This is actually the electron type of (anti-) neutrino. Subsequently two other varieties of neutrinos were discovered, the muon neutrino in 1962 by Schwartz, Steinberger and Lederman at Brookhaven National laboratory, USA [5] and the tau neutrino in 1999 by the DONUT collaboration at Fermilab, USA [6]. The detection of neutral current events at CERN, provided a very important verification of a prediction of the electro-weak (EW) theory of Steven Weinberg, Abdus Salam and Sheldon Glashow which apart from unifying the quantum theory of electrodynamics and weak interactions, also predicted the existence of the W^+ , W^- and Z^0 bosons, whose exchange between particles is responsible for the weak force (see Table1). This is analogous to photon exchange between charged particles giving rise to the repulsive or attractive Coulomb force. The EW theory field combined with a quantum theory for strong interactions called quantum chromodynamics (QCD), and the associated Higgs boson constitutes the standard model (SM) of particle physics (see Table 2 for the fundamental particles therein). One of the key ingredients of the SM is the Higgs. The Higgs field is responsible for giving mass to particles such as the electron and it has been discovered recently at the Large Hadron Collider (LHC) at CERN.

Neutrinos oscillate!

We now return to the phenomenon of neutrino oscillations. While the spin and electric charge of the neutrino are known, its rest mass is not. Only an *upper bound* can be placed by experiments, the

Table 1: Four basic interactions in nature

Type	Range	Force mediator	Relative strength	Example
Gravitational	Infinite	Graviton (?)	10^{-38}	Earth-Sun
Weak	10^{-18} m	W^\pm, Z^0	10^{-5}	β^\pm decay
Electromagnetic	Infinite	Photon	1/137	Hydrogen atom
Strong	10^{-15} m*	Gluon	1	Quarks in proton, nucleons in nuclei *range of nucleon - nucleon force

Table 2: Fundamental particles

Quarks			Electric charge	Mass (GeV)	Bosons mediating interactions [mass (GeV)]
u	c	t	+2/3	0.0023, 1.275, 173	
d	s	b	-1/3	0.0048, 0.095, 4.2	
Leptons					
ν_e	ν_μ	ν_τ	0	$<2 \times 10^{-9}, <1.7 \times 10^{-4}, 1.8 \times 10^{-2}$	
e^-	μ^-	τ^-	-1	$0.511 \times 10^{-3}, 0.106, 1.78$	

most stringent being that on the electron anti-neutrino of $\sim 2 \text{ eV}/c^2$. For comparison the rest mass of the electron is $511 \text{ keV}/c^2$. Although we do not yet know the mass(es) of the neutrino(s) we do know the mass differences, or more precisely, the difference(s) of the square of the masses. The possibility that neutrinos oscillate was first pointed out by Pontecorvo, a student of Fermi, in the mid-60s. A requirement of the phenomenon of neutrino oscillations is that at least 2 of the 3 known types of neutrinos have non-zero mass. If this is the case a neutrino, born as a particular type (e , μ or τ) propagates in space with the different mass states moving with different speeds. Since they are moving close to the speed of light (c), the relative differences in speed, measured on this scale, are small. Each flavor of neutrino has a different mix of neutrino mass states, decided by nature and parametrized in terms of 3 mixing angles, 3 differences in the square of masses and another angle related to the possibly different behaviour of particles as compared to antiparticles. At a certain distance from its birth an electron type neutrino may transform, chameleon-like, into a muon - or tau- type of neutrino. Such oscillations, also known as mixing, are seen in the strongly interacting particles at a much smaller level. As the late John Bahcall, an eminent astrophysicist who, with Ray Davis, proposed the radiochemical Chlorine detector for measuring solar neutrinos and calculated their expected flux leading to the solar neutrino problem, has put it -

Solar neutrinos have a multiple personality disorder. They are created as electron neutrinos in the Sun, but on the way to the Earth they change their type.

For neutrinos, the origin of the personality disorder is a quantum mechanical process, called "neutrino oscillations".

Interestingly, Bahcall's proposal that the observed shortfall in the measured solar neutrinos as compared to his calculations had a particle physics origin, viz. neutrino oscillations, was not taken seriously by the high energy physics community. His stand was however vindicated, first through observations on atmospheric neutrinos (described later) and then through a neutrino type or flavor blind measurement at the Sudbury Neutrino Observatory, a 1.7 km deep mine in Canada. The latter experiment used 1000 tons of pure heavy water and measured the flux of electron neutrinos as well as the sum of fluxes of all (active) neutrino flavours. The shortfall seen in the former flavor was made up in the latter and confirmed the conjecture of Bahcall.

Neutrino oscillations may be understood by first looking at the simpler two-flavour mixing. Let us look at an analogous situation in optics related to the propagation of light in a optical medium that has a 'handedness' in that it responds differently to left handed and right handed circularly polarized light. This results in rotating the plane of polarization of plane polarized light to the left (laevorotatory) or to the right (dextrorotatory). In a similar manner, the two mass states move at different speeds so that what started out as an electron neutrino looks partly like the muon neutrino as it propagates over space and returns to its original (electron neutrino) state at a distance characteristic of its energy and the quantity $m_2^2 - m_1^2$. Here m_1 and m_2 are the masses in the alternate description where masses

are definite, as opposed to the “electron-ness” or “muon-ness”. Using elementary quantum mechanics, the time evolution of a neutrino starting as one of say the electron type can be calculated in the 2-flavour mixing scenario. It can be shown that the survival probability is given by

$$P_{ee} = 1 - \sin^2 2\theta \sin^2 \left(\frac{1.27 \Delta m^2 L}{E} \right)$$

where θ is the mixing angle, E the neutrino energy in MeV, L is the neutrino propagation length in metres and Δm^2 in eV^2 . The angle θ (which is real) is used to parametrize the elements of the 2'2 mass mixing matrix that connects the leptonic and mass eigenstates through the relation

$$\begin{bmatrix} e \\ \mu \end{bmatrix} = \begin{bmatrix} \cos \theta & \sin \theta \\ -\sin \theta & \cos \theta \end{bmatrix} \begin{bmatrix} m_1 \\ m_2 \end{bmatrix}$$

Here e, μ are the two leptonic eigenstates and m_1, m_2 are the two mass eigenstates.

The more realistic 3-flavour case has more complicated expressions involving 3 mixing angles, analogous to the 3 Euler angles which are needed to connect 2 coordinate frames connected by rotations in 3D space. In addition there are 3 mass squared differences and one CP violating phase. *

The most compelling evidence for neutrino oscillations was obtained from measurements on atmospheric neutrinos. The neutrinos originate from the decays of the pion and the daughter muon. The pions are produced in cosmic ray interactions with ^{14}N and ^{16}O nuclei in the upper atmosphere. The pions then decay with a lifetime of about 26 nsec producing a muon and a muon neutrino and the muon in turn decays to an electron, muon neutrino and an electron neutrino. Thus for every pion decay there are 2 muon neutrinos and 1 electron neutrino. As this is the major source of atmospheric neutrinos, the ratio of the detected muon to electron neutrinos is model independent and therefore very robust. The Kamiokande I experiment found the expected ratio of muon to electron neutrinos for downward

* C changes particle to anti-particle, P stands for parity under whose operation $\mathbf{r} \rightarrow -\mathbf{r}$. CP symmetry implies invariance under the combined operations of C and P.

pointing events but a deficit, by about a factor of two, for upward pointing events. A natural explanation was that the upward going muon neutrinos change their flavor becoming tau neutrinos which are detected with much less efficiency as compared to muon or electron neutrinos.

Neutrino sources and experiments

There are several sources of neutrinos listed below (see Fig.2): (a) the sun [7] (b) cosmic ray interactions with the earth's atmosphere [8] (c) supernovae and other explosive events in universe [9] (d) particle accelerators such as at CERN in Geneva [5,10] (e) nuclear reactors [4] and (f) Geo-radioactivity [11]. Each has a characteristic energy range, flux or source strength and angular distribution (isotropic from source for most except the accelerator produced). The first ever detection of supernova neutrinos, from SN1987a, took place in 1987 by several detectors worldwide, chief among them being Kamiokande I which detected 11 of the total of 17 events. The beginning of neutrino astronomy was acknowledged by the award of a shared Nobel prize to Koshiba who led the Kamiokande experiment. This experiment had been designed to look for proton decay which it did not find, as nature did not oblige! On the other hand the background due to neutrinos turned out to be a rich mine viz. atmospheric neutrinos which led to the discovery of neutrino oscillations, the first real time detection of solar neutrinos including the direction of their source (the sun) and neutrinos from a stellar collapse SN1987a.

Man made muon neutrinos via in flight decay of pions were first detected by a team led by Schwartz, Lederman and Steinberger in 1962 at Brookhaven National Lab. All three received the Nobel prize in the year 1962 for this discovery. The same method was used with more powerful accelerators and using the off axis decay to produce quasi-mono-energetic muon neutrinos to do several measurements. If the pions are relativistic (speed \approx speed of light) the neutrinos travel in a narrow cone whose angle is small enough to allow experiments to be done at

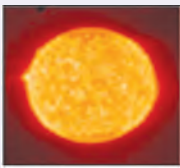





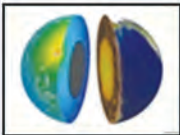
Source		Energy	Flux/Number
Sun		0-15 MeV	$6 \times 10^{10} /(\text{cm}^2.\text{s.})$
Nuclear reactors		0-10 MeV	$2 \times 10^{20} /(\text{GWth.s.})$ from core
Particle accelerators		10-100 GeV	upto $10^{15} /\text{s.}$
Atmospheric neutrinos		0.5 – 20 GeV	$10^3 /(\text{m}^2.\text{s.})$
Supernova (stellar collapse)		5 – 100 MeV	10^{60} over about 10s.
Cosmic Big Bang		200 μeV	$330/\text{cm}^3$
Geo-neutrinos		0-4 MeV	$6 \times 10^6 /(\text{cm}^2.\text{s.})$

Fig. 2: Various sources of neutrinos (Courtesy: Google Image)

distances of the order of hundreds of kms. A state of art experiment is that of the MINOS collaboration where the neutrinos are produced at Fermilab and are measured 732 kms away in a mine by a 5.2 kton iron calorimetric detector. This experiment has measured the value of Δm^2 and $\sin^2 2\theta$.

The India based Neutrino Observatory (INO)

As mentioned before, atmospheric neutrinos were first detected in the deepest operating mine of its time, Kolar Gold Fields, by a TIFR-Osaka-Durham collaboration. The TIFR group later built a detector

to search for the pressing question of the time viz. do protons decay? This group was the first to publish results on this important question. However building larger detectors (than the 600 ton iron calorimetric detector) in the mine, especially at the deepest level which is the ideal location, was not possible. As it turns out protons have not yet been found to decay, with detectors worldwide that are 100 times larger. Also the KGF became economically less competitive compared to other gold mines and were eventually closed down. Meanwhile, around the late 90's, there began an effort to revive the experimental culture in

India and focusing on non-accelerator experiments in an underground laboratory. Building such a lab at the end of a tunnel, such as at Kamioka in Japan and Gran Sasso in Italy, was a better option for housing large detectors. At around this time the field of neutrino physics was becoming very interesting in view of results from the Kamiokande-I and Irvine-Michigan-Brookhaven experiments, which turned the background for proton decay (for which only upper bounds could be placed) measurements into a signal for atmospheric neutrino oscillations!

The idea of building an underground laboratory in India began with the signing of a MoU by the directors of 6 institutes of the Department of Atomic Energy in 2002. Early on it was decided that we build a 50-100 kton magnetized iron calorimeter (ICAL) to measure atmospheric neutrinos. This would be unique in that it would have the capability of distinguishing between neutrino and anti-neutrino induced events using the so called charged current interactions which produce muons of opposite charge. A similar proposal, MONOLITH, had been considered by an Italian group with a somewhat smaller detector of 32 kton. Simultaneously, R&D was begun on simulations (both for neutrino detection and the magnet) and the active detector element viz. glass Resistive Plate Chamber (RPC), a position sensitive, fast gas detector. It was envisaged that after some ground work a project report would be prepared. This was done in May 2006 [12] and reviewed by 6 international referees. The overall rating of the project was high with an advice that the project be implemented quickly.

The INO will be an underground laboratory located in Pottipuram, about 110 kms to the west of Madurai, at the end of a 2 km long tunnel with about 1 km rock cover all round (see Fig. 3 for a bird's eye view of the project). This will reduce the cosmic ray background by about a factor of a million enabling low background experiments to be carried out. While the ICAL detector for measuring atmospheric muon neutrinos will be the largest in

the underground laboratory, there are at least two other experiments which make use of the low cosmic background to search for neutrinoless double beta decay in ^{124}Sn and a silicon detector for directly detecting dark matter particles. Both will be based on cryogenic bolometers operating at temperatures of about 10 milli-Kelvin and are presently in the R&D phase at TIFR and SINP, respectively.

The main scientific goals [of the ICAL experiment are (i) the determination of the ordering of neutrino masses, known as the mass hierarchy problem viz. whether $m_3 > m_2 > m_1$ (normal hierarchy) or $m_2 > m_1 > m_3$ (inverted hierarchy) (ii) a more precise measurement of the mixing parameters θ_{23} and Δm_{23}^2 (iii) confirm (iii) search for explanation of anomalous Kolar events and possibly (iv) together with long baseline accelerator experiments address the very fundamental problem of the predominance of matter over antimatter in the universe [14]. The ICAL detector is best suited for making measurements of muons, and hence of, primarily, muon neutrinos.

The hierarchy sensitivity of the ICAL detector, which has a discovery potential, has its origin in the "matter effect" where the effective neutrino mass and mixing angles change when neutrinos propagate through any material such as the earth. The change is different for neutrinos and antineutrinos, something which can be used in measurements which can discriminate between the two such as those with the magnetic calorimeter ICAL. The large range of energies (1-10 GeV) and propagation distances (1-13000 km) of atmospheric neutrinos and the ability of ICAL to separately measure neutrinos and anti-neutrinos enables a very important problem of mass ordering, known as the mass hierarchy problem, of neutrinos to be addressed. We know from solar neutrino experiments that the mass eigenstate $m_2 > m_1$ but we do not know from experiments whether $m_3 > m_1$, m_2 or $m_3 < m_1$, m_2 . It should be mentioned that $\Delta m_{21}^2 = m_2^2 - m_1^2$ is about 30 times smaller than Δm_{32}^2 . Other detectors working in conjunction with accelerators are plagued with an ambiguity problem whereby for certain values

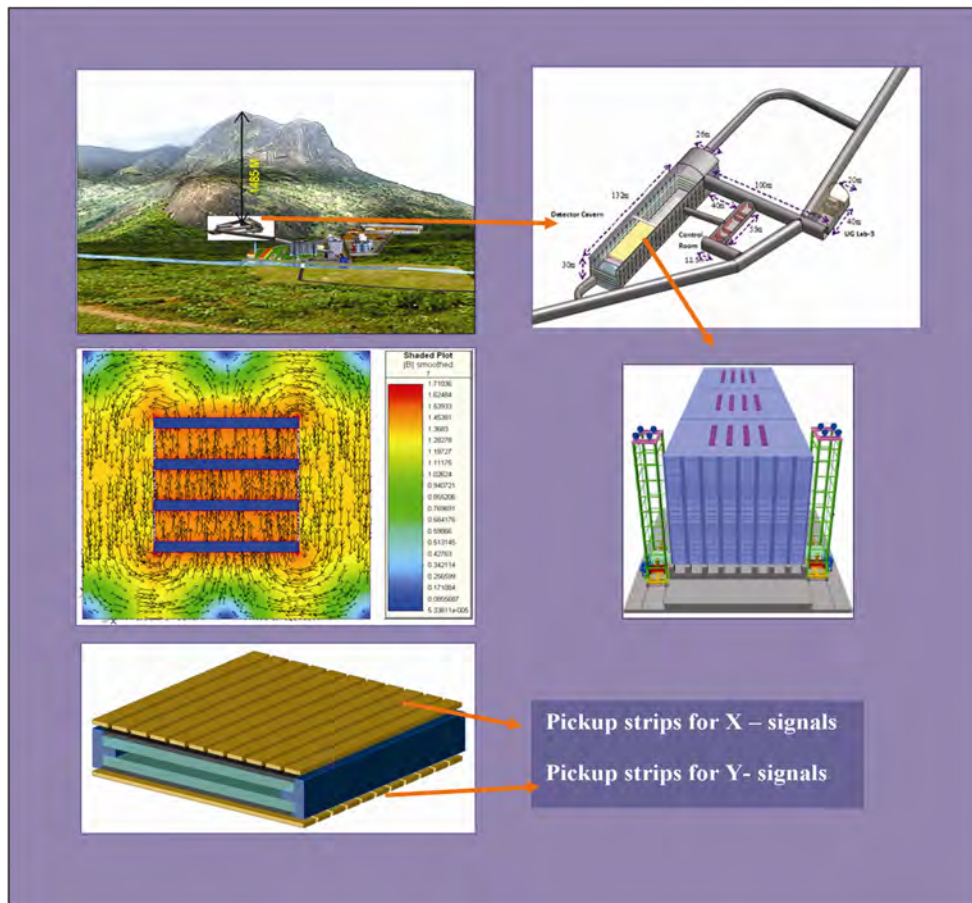


Fig. 3: From top left clockwise (a) view of the mountain inside which the INO caverns will be located (b) cavern complex (c) schematic of ICAL magnet with RPC handling trolleys (d) schematic of glass RPC with glass gap, graphite coating for application of high voltage and pickup strips on either side of gap in X- and Y-directions (e) simulated magnetic field across 16m×16m area. The color code indicates the B-field strength in Tesla.

the parameter which quantifies the CP violation (related to the different behavior of neutrino and anti-neutrinos) in the neutrino sector there is no sensitivity to the mass hierarchy. On the other hand if the results of ICAL and accelerator based experiments such as Nova using the Fermilab neutrino beam and T2K could yield a definite answer whether the CP symmetry is violated in the neutrino sector, and if so, whether it is enough to explain the matter-antimatter asymmetry in the universe.

The precision measurement of Δm_{32}^2 and $\sin^2 2\theta_{23}$ is another goal of ICAL. Similarly a handful of events, the so called Kolar events, have been observed in the KGF experiments (~1965-1990) at depths of about 2.3 kms. At these depths cosmic ray muons

constitute a negligible background. These anomalous events were then ascribed to a new particle produced in neutrino-rock interactions which emerges from the rock to decay in the air volume. This should then have been seen in accelerator which turned up negative. A possible recent explanation [15] could be verified at INO.

References

1. How weak is the weak force? For example, the weak force between a proton and the neutron in a nucleus is about 10^{-14} times weaker than the strong force which is responsible for binding the nuclear constituents. W. Pauli, H.A. Bethe (another Nobel prize winner who proposed the fusion

reaction as a power source of the stars including the sun) and R. Peierls had predicted that it would be impossible to detect because of its extremely low probability of interaction with matter.

2. The weak interaction is one of the 4 basic interactions in nature, the other three being the strong interaction (which binds nucleons in a nucleus or quarks in a proton or neutron, for example), the familiar electromagnetic interaction (which binds atoms and molecules, and which helps mobile communication) and gravitational interaction (which gives us weight and holds the earth in its orbit around the sun).
3. E. Fermi, *Ricerca Scientifica*, 2, No. 12 (1933); *Z. Phys.*, 88, 161 (1934). An English translation by Fred L. Wilson, can be found in "Fermi's Theory of Beta Decay", *Am. J. Phys.* 36 (1968) 1150. Interestingly, Fermi's paper was first submitted to *Nature* which rejected it. The journal later acknowledged this decision as one its greatest blunders.
4. C.L. Cowan, F. Reines, F.B. Harrison, H.W. Kruse, A.D. McGuire, "Detection of the free neutrino: a confirmation", *Science*, 124 (1956) 103-104. Reines has recalled that he first toyed with the idea of detecting neutrinos from the atomic bomb of the Manhattan Project at Los Alamos. He was persuaded by Luis Alvarez to look for a more steady and enduring source of neutrinos such as a nuclear reactor! Nuclear reactors have also been used to produce strong radioactive sources such as ^{51}Cr for calibrating the Gallex, Sage and GNO detectors built to measure solar neutrinos using ^{71}Ga as the probe nucleus.
5. G. Danby, J-M. Gaillard, K. Goulianos, L.M. Lederman, N. Mistry, M. Schwartz, J. Steinberger, "Observation of high-energy neutrino reactions and the existence of two kinds of neutrinos", *Phys. Rev. Lett.* 9 (1962) 36-44.
6. K. Kodama et al., "Observation of tau neutrino interactions", *Phys Lett. B* 504 (2001) 218-224. The DONUT collaboration found the first evidence for the tau neutrino at Fermilab.
7. R. Davis, Nobel Lecture: A half-century with solar neutrinos, *Rev. Mod. Phys.*, 75, (2003) 985-994; J.N. Bahcall, "Solar neutrinos. I. Theoretical", *Phys.Rev. Lett.* 12 (1964) 300-302.; J.N. Bahcall, M.H. Pinsonneault, and S. Basu, "Solar models: current epoch and time dependences, neutrinos, and helioseismological properties," *Astrophys. J.* 555 (2001) 990-1012.
8. First discovered in an experiment at the Kolar Gold Fields by a TIFR-Osaka-Durham collaboration. C.V. Achar et al, *Phys. Lett.* 18 (1965) 196-199.
9. K. Hirata et al. (Kamiokande II collaboration), "Observation of a neutrino burst from the supernova SN1987A" , *Phys. Rev. Lett.* 58 (1987) 1490-1493; R.M. Bionta et al. (IMB collaboration), *Phys. Rev. Lett.* 58 (1987) 1494-1496.
10. P. Adamson et al. (MINOS collaboration), *Phys. Rev. Lett.* 101 (2008) 131802-1:5.
11. T. Araki et al., "Experimental investigation of geologically produced antineutrinos with KamLAND", *Nature* 436, (2005) 499-503.
12. INO Report (2007) and the INO website www.ino.tifr.res.in
13. It may mentioned that quite often the stated goals may not necessarily be achieved because of the very nature of scientific research. On the other hand state of art instruments sometimes unearth phenomena that were not anticipated at the start of the project. One such examples is the Japanese water Cerenkov detectors at Kamiokande which were built to search for proton decay, did not find it, but turned the background from neutrinos into signals that lead to the discovery of neutrino oscillations using atmospheric neutrinos.

14. A.D. Sakharov, "Violation of CP invariance, C asymmetry and baryon asymmetry of the universe", *JETP Lett.* 5 (1967) 24-27. Sakharov was the first to point out that the matter-antimatter asymmetry in the universe can arise only if 3 conditions are met viz. (a) non-equilibrium conditions (b) baryon non-conservation (c) CP violation.
15. M.V.N. Murthy and G. Rajasekaran, "Anomalous Kolar events revisited: Dark matter?", *Pramana*, 82 (2014) L609-615.

Seamless Access to Networked Information: The Role of Domain Ontologies

Sangeeta Deokathey and K. Bhanumurthy
Scientific Information Resource Division

Abstract

In the current information overload mode, access to the right kind of information is even today an uphill task. This is because of complexities both in the types of documents and in the information contents of the documents. Providing seamless access to networked information through a single platform is still achievable, through the use of Domain Ontologies. The present article provides basic information on Domain Ontologies, how they can be developed and a flavor of R&D activities at the Scientific Information Resource Division on Domain Ontologies.

Introduction

We live in a world of information. Einstein [1] reinstated its importance when he said "Know where to find the information and use it; that is the secret of success". According to Horowitz [2], American Information Scientist, "Not having the information you need when you need it, leaves you wanting. Not knowing where to look for that information leaves you powerless. In a society where information is King, none of us can afford that".

We live in an information society. Apart from the traditional disseminators of information, such as the mass media, the scientific and technical publishing houses and learned societies, there is now a new medium of mass communication: the Internet. It is turning the entire gamut of writing, publishing and copyright issues, upside down. Libraries and Information Centres, have been providing and continue to provide information services to their clientele, in this ever changing scenario.

Knowledge Organization (KO)

Organization of Knowledge for effective retrieval is one of the most important functions of an Information Centre. Every information system uses two distinct schema for encoding information

embodied in a document. One represents the subject contents of a document through the use of a classification scheme, a thesaurus or a subject heading list etc., the other provides descriptive information about a document like title, author, publisher, etc. These are handled by metadata schema. The main problem in the context of interoperability is that, a subject schema used in one library may not be compatible with that of another library. If a piece of information is downloaded from the Internet, it is represented in an entirely different schema. Therefore, achieving semantic homogeneity in heterogeneous digital information resources is a real challenge.

The electronic era, the Internet and the subject approach to information

Advances in Internet-based information services, have further precipitated the need, to organize information in a more effective way. As far as indexing and vocabulary control methods are concerned, there is no standardization of terminology on the web. A number of research methods and experiments are currently on, to create a semantic web; a semantic interlinking of all the information on the web. These methods include

the use of free text, i.e. “key words” taken from the text, clustering methods based on statistical co-occurrence of words, linguistic methods using semantic clustering and neural network methods for browsing and searching the web.

Current scenario in Knowledge Organization

Digital information explosion, has necessitated the growth and development of new indexing tools and systems. Several efforts have been made to use Classification schemes to organize digital information, both in Libraries and Information Centres and on the Internet. Controlled Vocabularies and Natural Language Indexing Systems continue to be used by many database systems on the Internet. But, these systems are one-dimensional in their approach, i.e. concepts or keywords have a one-to-one correspondence among themselves. This approach was feasible in the case of traditional subjects, represented by these systems, over the years. But now, subject areas are no longer clearly delineated. There is an intermingling of other subjects. For e.g. Bioinformatics, in which, Biology, Computers and Technology have fused together, as one compound, interdisciplinary subject. In such a scenario, a one-to-one correspondence between concepts/keywords will not provide an accurate representation of the subject contents of a document. A one-to-many correspondence between concepts or keywords becomes the norm and this correspondence needs to be brought out during concept mapping and indexing. A whole new vocabulary needs to be developed, to semantically map the entire subject field. Creating a subject-specific indexing tool such as a Thesaurus is time-consuming, requires subject expertise and is difficult to update regularly.

Ontologies

An Ontology provides an answer to these problems. It is multidimensional in its approach to organizing information. Any number of linkages (relationships) can be provided for each concept or keyword as and when required, since it is a continuously

evolving, dynamic system. An Ontology is also more amenable to the addition of new concepts as there is no need for developing a rigid vocabulary, which has to be strictly adhered to, both during indexing and searching (as in the case of thesauri). An Ontology makes use of both standard terms and free-text terms, with the result that updating is almost immediate. A user is free to suggest any new concept that he/she feels is important and is relevant to the subject. Ontologies are increasingly being used as KO tools, especially for digital information and web-based information services.

Ontologies and Philosophy: According to the Oxford English Dictionary the first recorded use of the word “Ontology” in English, was in year 1721. Ontology (ontos = being and logos = study) means “the study of being”. It is the theory of objects and their ties. Traditionally, Ontology as a subject, was the focus of Philosophers and Logicians who used the term to denote the study of what is, i.e. what exists, the kinds and structures of objects, properties and other aspects of reality of the universe. Ontology is the first part that actually belongs to Metaphysics. It is a pure doctrine of elements of all our *a priori* cognitions; or it contains the summation of all our pure concepts that we can have *a priori* of things.

Ontologies and Artificial Intelligence: In the field of Artificial Intelligence, an Ontology is a theory concerning the kinds of entities and specifically the kinds of abstract entities, that are to be admitted to a language system. The concept was developed and implemented since the early 1990s. AI researchers use Ontologies (in plural) for two basic purposes: Problem Solving Methods (PSMs) and Knowledge Based Systems (KBSs). One of the most popular definitions of Ontologies is by Gruber [4]: an Ontology is “a formal explicit specification of a shared conceptualization”.

Ontologies and the Semantic Web Initiative by the W3C: The ultimate goal of the Web is to enable computers to do more useful work and to develop systems that can support trusted interactions

over the network. The term “Semantic Web” refers to W3C’s vision of the Web of linked data. The Semantic Web is the communication platform between computers and people operable via semantically encoded information. It is an extension of the current Web, in which meaning of information is clearly and explicitly linked from the information itself, better enabling computers and people to work in cooperation. Ontologies are an integral part of this communication platform.

Ontologies and Information Science: In the context of Information Science, an Ontology is yet to be formally defined. As of now, Ontology is still an evolving concept and a consensus is yet to be reached on the exact definition. Therefore the authors have evolved a **working** definition of a domain ontology for the purpose of developing new domain ontologies.

“A domain ontology is a Knowledge Organization tool on any subject domain either pure, interdisciplinary or multidisciplinary and which incorporates both a metadata schema and a

vocabulary. It is based on WWW standard for metadata encoding and is thus interoperable in any digital environment either intranet or Internet. It uses both available controlled vocabulary terms and free index terms and is based on the concept of Literary Warrant”.

Types of Ontologies

According to Gruber’s definition of an Ontology, it is “a formal explicit specification of a shared conceptualization”; ‘Formal’ refers to the fact that an Ontology should be machine readable. ‘Explicit’ means that the types of concepts used and the constraints on their use should be explicitly defined. ‘Shared’ implies acceptance and use of consensual knowledge by the participating groups. And finally, ‘conceptualization’ refers to an abstract model of phenomena in the world through identification of relevant concepts of those phenomena. AI researchers have classified Ontologies using different criteria.

According to van Heijst [5], Ontologies can be classified into two main types as seen in Fig. 1.

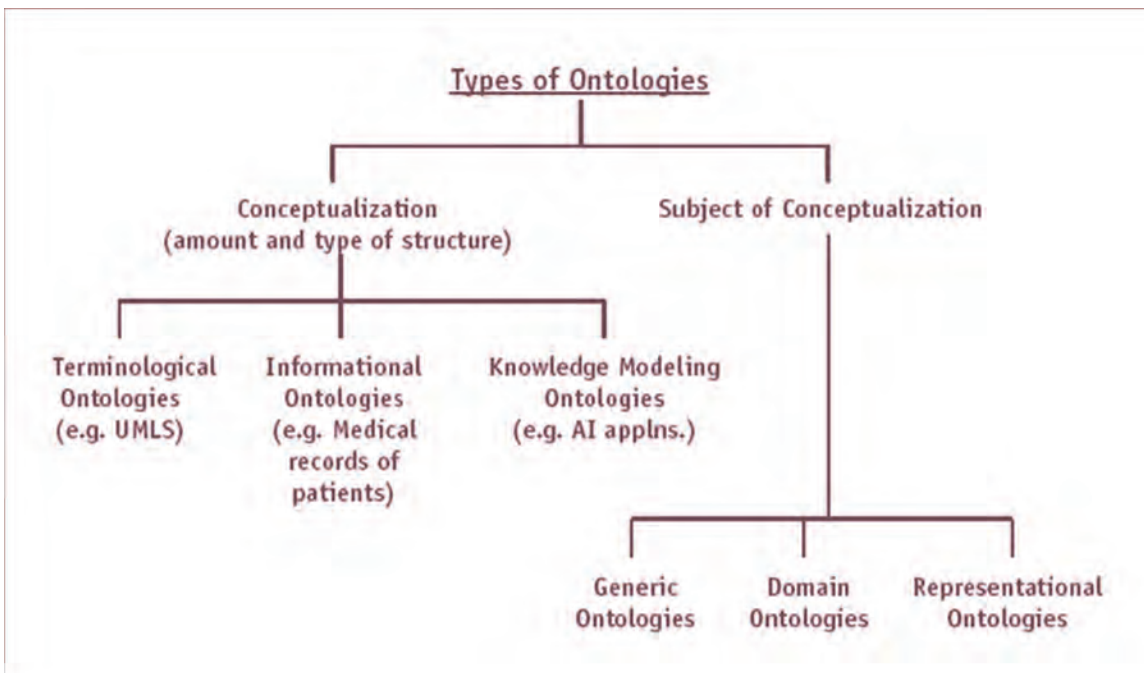


Fig. 1: Ontological types (van Heijst [5])

Terminological Ontologies such as Unified Medical Language System (UMLS) of the National Library of Medicine (NLM), **Informational Ontologies** which specify the record structure of databases, for e.g. the medical records of patients and **Knowledge Modelling Ontologies** (for AI applns.) fall under the first type. **Domain Ontologies** that express conceptualizations specific for a particular domain, **Generic Ontologies** that are general in nature and **Representational Ontologies** fall under the second type.

Ontology language

Whatever the type of Ontology, every Ontology has to be represented by a predefined machine language. The current Ontology representation languages are of three types:

1. **logic-based** (using First Order Logic)
2. **frame-based** (using Frame Logic) and
3. **web-based** (using RDF, XML, HTML format).

An Ontology language should ideally incorporate the advantages of all the three types of languages.

Ontology Development Methods

The basic difference between conventional Knowledge Organization & Retrieval tools and ontologies is the ease with which relationships between keywords, either free-text or controlled can be specified and the ease with which value addition can be accomplished through deeper semantics, in describing digital objects, both conceptually and relationally. If one wants to develop a domain ontology, the entire domain needs to be mapped semantically in the form of a network, to better understand the linkages between different concepts in a domain. For instance, in a thesaurus, only three types of relationships can be expressed: Hierarchical, Equivalence and Associative. Through domain ontologies, Associative, Lateral or Related term relationships can be better expressed. This is particularly important in developing domain ontologies in fast growing, interdisciplinary subject areas, where related term relationships are significant

for search and subsequent retrieval of information. Thus domain ontologies, tailored to the KO&R needs of a particular organization or user community, can be specifically created by ontology developers. The process of conceptualization is at the core of developing domain ontologies [6]. Conceptualization is done through the identification and interlinking of keywords/descriptors in the selected domain. A keyword in combination with other keywords semantically related to it is transformed into a more comprehensive 'concept'. Using theoretical principles of classification, keywords can be converted into semantically-rich concepts through generation of one-to-many correspondences or linkages between them. These associations or linkages are developed according to user requirements by the ontology developers. Thus each domain ontology is unique since it represents a part of the reality of the universe conceptualized by it. Concept mapping is an intellectual process wherein basic knowledge about the domain as well as a deep understanding about the needs of the user community is required.

Development of Domain Ontologies at BARC

The multidisciplinary nature of research at BARC is an ideal platform for developing domain ontologies; as the current Knowledge Organization tools used at SIRD are uni-dimensional in their approach to information.

1. One of the areas selected for developing a domain ontology was Accelerator Driven Systems (ADS). Three select areas in ADS were identified: 1, ADS (general) 2. Accelerator Driven Transmutation and 3. Energy Amplifier. In consultation with Senior Scientists of BARC, a prototype was developed. Fig. 2 shows a schematic representation of a domain ontology. Following was the methodology:
 - a. Identification of appropriate concepts and keywords on ADS, using content analysis
 - b. Listing of the selected concepts and keywords on ADS, which had a threshold level of more than 2

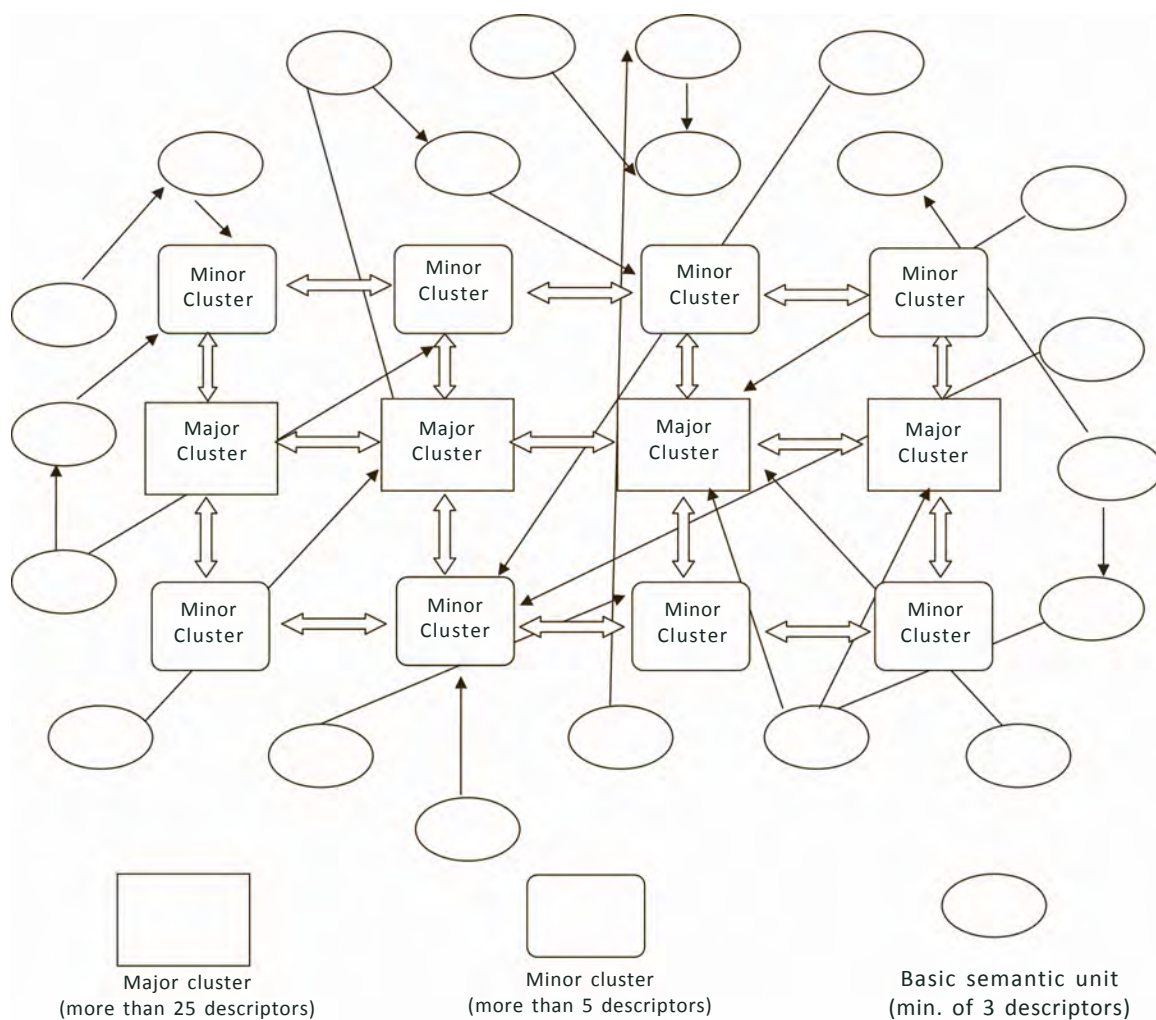


Fig. 2: Domain Ontology: a Schematic Representation (Deokattey et al. [6])

- c. Developing clusters of the select keywords on the basis of frequency count, using cluster analysis
 - d. Generating a one-to-many correspondence between the keywords using Facet analysis and thus interlinking them
 - e. Developing a semantic network of selected concepts and keywords on ADS and concluding the conceptualization process
 - f. Uploading the above semantic network onto a web-based platform, developed for the purpose
 - g. Converting the bibliographic details of references on ADS into HTML format
 - h. Developing separate files on the three select areas of ADS and providing a link to the home page
 - i. Developing a home page for the domain ontology on ADS, with provisions for data security
 - j. Developing the prototype model of the domain ontology and testing and validating it.
2. A pilot study for developing a domain ontology for a micro-domain - Test Blanket Module (TBM) (an integral part of fusion reactors), was also undertaken at SIRD. Sample data downloaded from the INIS database yielded 1115 unique DEI (indexer-assigned) descriptors assigned to 548 records on TBM. Using the principles of co-word and facet analysis, a total of 31 core descriptors were selected for conceptualization. This method can be easily replicated to generate semantic networks and also in query expansion during search and retrieval

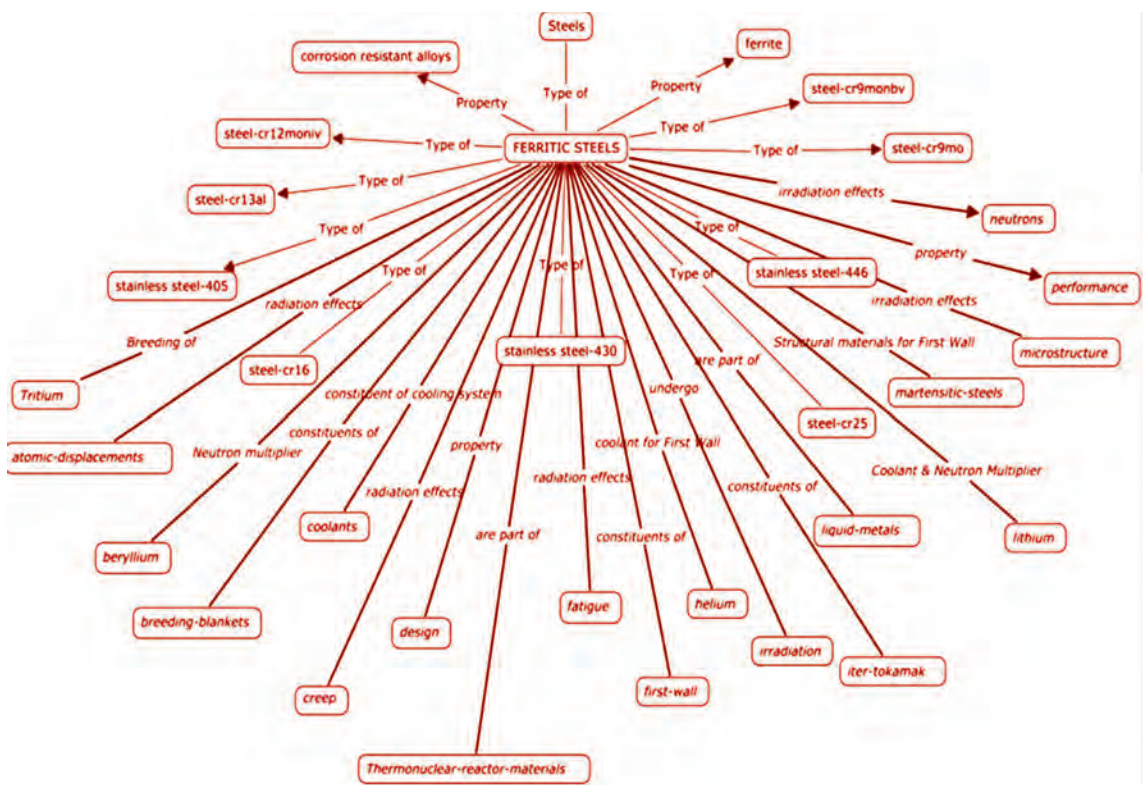


Fig. 3: A concept map for Ferritic Steels [3]

particularly in interdisciplinary subject domains. Fig. 3 is a graphical representation of the concept “Ferritic steels”, an important candidate material for the TBM.

3. Presently, a proposal is being developed to generate reusable modules of domain ontologies in core areas of R&D at BARC.

Conclusion

In the context of Information Science, Ontologies are still at a nascent stage. If a domain Ontology has to be developed, the first requirement would be, that it should be based on the concept of literary warrant; which means that only domain knowledge would be utilized to develop an ontology. Secondly, in the present era of reusable modules of ontologies for various applications, interoperability is a major issue; which means an ontology should be very flexible and yet be web-enabled. Third and the most important area is vocabulary control. Information Scientists need to think beyond Classes, Keywords and Descriptors to represent information, embodied

in any document. The basic idea or the Concept as envisaged by Hjørland [8], would be the key to effective organization and retrieval of knowledge. A concept encompasses keywords, descriptors and their corresponding linkages. These linkages should also take into account, institutional, cultural and national warrants. The complexity of evolving subject domains is another problem area and innovative methods, including webometric techniques, need to be used to harness concepts, for developing ontologies in interdisciplinary domains. The theoretical foundations of Classification, rooted in Logic and Cognitive Psychology, can form the ideal basis for developing appropriate techniques and methods [3,7] for creating new domain ontologies.

References

1. ThinkExist.com Quotations, “Albert Einstein Quotes”; available at <http://www.ThinkExist.com>.

2. Available at <http://www.nonstopenglish.com/reading/quotations>
3. Deokattey, Sangeeta; Dixit, D.K. and Bhanumurthy, K. Co-word and Facet analysis as tools for conceptualization in Ontologies; a preliminary study of a micro-domain. (pp153-158) In: Neelameghan, A. & Raghavan, K.S. (Eds.): Categories, Contexts and Relations in Knowledge Organization: Proceedings of the 12th International ISKO Conference, 6-9 Aug., 2012, Mysore, India. Wurzburg, Ergon-Verlag, 2012.
4. Gruber, T.R.: Towards principles for the design of Ontologies used for Knowledge Sharing. *International Journal for Human Computer Studies*, 43, (5/6), 1995, pp.907-928.
5. van Heijst, G., Schreiber, A.T. and Wielinga, B.: Using explicit Ontologies in KBS Development. *International Journal of Human Computer Studies*, 46, 1998, p.184.
6. Deokattey Sangeeta, Neelameghan A. and Vijai Kumar: A method for developing a domain ontology; case study for a multidisciplinary subject. *Knowledge Organization*, 37 (3), 2010, pp.173-184.
7. Deokattey Sangeeta and K. Bhanumurthy. Domain Visualization Using Concept Maps: A Case Study. *DESIDOC Journal of Library & Information Technology*, 33 (4), July 2013, pp. 295-299.
8. Hjørland, B.: Concept Theory. *Journal of the American Society for Information Science*, 60,2009,pp.1519-1536.

Theme Meeting on Challenges in Fast Reactor Fuel Reprocessing (CFRFR-2014)

A theme meeting on “Challenges in fast reactor fuel reprocessing” was organised at AFFF Lecture Hall, BARC, Tarapur on October 18, 2013. The meeting was organized by Indian Association of Nuclear Chemists and Allied Scientists, Tarapur chapter in association with Board of Research in Nuclear Sciences (BRNS), Department of Atomic Energy, Government of India. The welcome address was given by Shri. Mohd. Afzal, Head A3F and chairman, IANCAS Tarapur chapter. The meeting was inaugurated by Dr. K.L. Ramakumar, Director, Radiochemistry and Isotope Group and President, IANCAS, Mumbai. In his inaugural speech, Dr. Ramakumar emphasized on the nuclear material accounting issues encountered in nuclear process on every stage. He stressed that handling of large amount of fissile materials and its losses during reprocessing and fuel fabrication should be taken care due to their strategic importance. He also emphasized that the theme of the topic is very relevant in view of the current thrust area for the scientists and engineers as PFBR is on the verge of implementation with MOX fuel shortly. Shri. Arun Kumar, Director, Nuclear Fuels Group acquainted the audience with the important aspects and associated challenges in fuel fabrication for fast reactors. He specially mentioned the MOX solid waste residuals and the recovery of plutonium from such waste.

The meeting was divided into two sessions. In Session-I, eminent speakers from various units of DAE delivered their lectures. Shri R. Natarajan, Director, Reprocessing

Group, IGCAR, Shri. Arun Kumar, Director, Nuclear Fuels Group, BARC presented the invited lectures. Shri K. Nagrajan, Associate director, Chemistry Group, IGCAR, Dr. P.N. Pathak, RCD, BARC and Shri. Y. Kulkarni, CS, TNRPO delivered invited talk in second session. A number of challenges were discussed by speakers with regard to engineering and physical design, safety assessment, chemistry challenges encompassing the entire nuclear fuel cycle starting from front end stage of fuel fabrication to back end of fuel reprocessing and waste management aspects.

In the concluding session, a panel discussion was conducted where Dr. K.L. Ramakumar, Director, RC&I Group, Shri Arun Kumar, Director, NFG, Shri R. Natarajan, Director, Reprocessing Group, IGCAR, Shri. Y. Kulkarni, CS, TNRPO and Shri. Mohd. Afzal, Head, AFFF and Chairman, IANCAS, Tarapur chapter participated. Shri. Arun Kumar focused the importance of waste management as waste managers are the part of fuel fabrication facilities in upcoming projects. Dr. Natarajan emphasized on remotization of the facilities to minimize neutron and radiation dose to the workers. Shri. Y. Kulkarni addressed the limits of neutron dose limits. He suggested to provide the plant level facility to test the alternate extractants in every aspects to be encountered in FBR fuel reprocessing.

Dr. Ramakumar appreciated the efforts of IANCAS Tarapur Chapter for bringing together the experts from different centres of DAE for the theme meeting.



Dr. K.L. Ramakumar, Director, Radiochemistry and Isotope Group and President, IANCAS, delivering the inaugural address.

Shri. Arun Kumar, Director, NFG, Dr. K.L. Ramakumar, Shri Mohd. Afzal, Head, A3F *Director, GSO, Shri Y. Kulkarni, CF, TNRPO at the concluding session.

Technology Transfer to Industries

During the period between March 2014 and September 2014, BARC has transferred eight technologies to various industries. Technology Transfer & Collaboration Division (TT&CD) co-ordinated these technology transfers. The details are given below:

A. "Portable Radioisotope Identification (PRID)" technology was transferred to M/s. Nucleonix Systems Pvt. Ltd., Hyderabad (A.P.) on 04.03.2014.

The Portable Radioisotope Identification (PRID) system developed by Electronics Division detects and identifies multiple radionuclides, provides quantified results using field strength analysis and stores the results & spectrum for future reference. It can be operated in various modes as Identifier mode, MCA mode, Transfer stored spectrum mode, Administrator mode and Dosimeter mode. It has ability to identify up to 20 Radionuclide (easily expandable). It has 15 hours continuous operation battery life.

The Portable Radioisotope Identification (PRID) finds applications for ascertaining radioactive contamination mainly for public safety. One of the applications in steel industry is ore and scrap handling.



Standing from left are Sh. Shiv Kumar, ED, Sh. J. Nishant Reddy, Director (IT), Nucleonix Systems Pvt. Ltd, Sh. V.B Chandratre, Head, Microelectronics Section, ED, Dr. Anant Krishnan, Head, ED, Sh. Narendra Reddy, MD, Nucleonix Systems Pvt. Ltd, Sh. C.K Pithawa, Dir. E&IG, Sh. G. Ganesh, Head, TT&CD and Smt. Preeti K Pal, TT&CD

B. "Preparation of Thin Film Composite (TFC) Charged Nanofiltration (NF) Membranes" technology was transferred to M/s. Osmotech Membranes Pvt. Ltd., Rajkot, Gujarat on 07.03.2014

This technology developed by Desalination Division refers to a novel process for preparation of Thin Film Composite (TFC) Charged Nanofiltration (NF) Membranes containing surface negative charge in the form of fixed sulfonic acid ($-SO_3^-H^+$) groups. An interesting feature of these membrane is the huge



Standing from left are : Dr. T.K Dey, DD, Dr. R.C Bindal, Head, MDS, DD, Sh. Jaman Vagadia, MD, M/s. Osmotech Membranes Pvt. Ltd, Sh. G. Ganesh, Head, TT&CD, Sh. Bhavesh Bhuva, Smt. Preeti K Pal, TT&CD

difference between the solute rejections for high rejecting solutes (Na_2SO_4 : 96 %) and low rejecting solutes (NaCl : 25%) which enables the membranes fractionally separate them when they are present together in a mixture.

This technology has tremendous potentials for applications in aqueous stream separations such as in production of potable water from partially brackish hard water, removal of heavy metal contaminants, removal of microbial (bacteria/virus) contaminations,

pretreatment of saline water for desalination processes like RO and MSF, and a host of other areas like pharmaceuticals and bio technological industries, downstream processing, food and beverage industries, dairy industry, waste water treatment.

C. "Nanocomposite Ultrafiltration Membrane Device for Domestic Drinking Water w.r.t. Arsenic, Iron & Microbial Contaminations" Technology was transferred to two parties (1) M/s. Rupali Industries, Mumbai on May 9, 2014 and (2) M/s. SONADKA, Mumbai on June 16, 2014.

Desalination Division (DD) has developed a methodology to produce a domestic water purification device which is made of polysulfone based nanocomposite ultrafiltration membrane in cylindrical configuration. This device can be effective for removal of microbial contaminations and decontamination of arsenic and iron through chemical addition without the need of any electricity and overhead water tank, and hence can be used even in slums and rural areas of the country. The contamination level is reduced below the permissible limits as specified by IS 10500 for drinking water standard.

D. "Mass Multiplication Medium for Biofungicide Trichoderma Spp." Technology was transferred to M/s Ajay Biotech (I) Ltd., Pune on 20.5.2014

This technology has been developed by NA&BTD. The field applications of Trichoderma spp. require mass multiplication which can be done using solid as well as liquid state fermentation. In the industrialized nations, liquid fermentation is extensively used for multiplication of Trichoderma spp. for commercial formulation. A low cost mass multiplication medium for faster growth of Trichoderma spp. is developed. This material supports better growth of

biofungicide compared to existing methods and addition of synthetic sticker is not required while making its formulation. The process is cheaper than the existing methods and is based on the material which is inexpensive and available locally. Hence, in true sense this technology generates wealth from waste.

E. "Process for Retaining Pericarp Colour and Extending Shelf Life of Litchi" technology was transferred to M/s SCRIMAD, Madagascar, on 03.06.2014.

Litchi is a highly perishable commodity which remains fresh only for 2-3 days after harvest. India produces nearly 500,000 tons of litchi second only to China. Because of poor shelf life of litchi it cannot be transported to distant markets in India, also cannot be exported due to shelf life and quarantine barriers. Food Technology Division, BARC has developed a technology based on dip treatment using GRAS (Generally Recognized As Safe) chemicals which extends the shelf life of litchi fruit up to 60 days while maintained at 4^o C retaining its appealing pinkish-red color.

M/s SCRIMAD is a Madagascar based international trading company operating since 1998 in the Madagascar litchi industry. It is a member of the Groupement des exportateurs de Litchi de Madagascar (Group of Exporters of Madagascar Lychee), and markets the brand "MADPREMIUM Lychee". During the transfer of the technology, Dr. Sekhar Basu, Director, BARC, discussed about the prospects and benefits of this technology for litchi



Dr S Gautam, FTD, Mr S Rakotondraohva, M/s SCRIMAD, Dr N Khalap, TT&CD, Dr S K Apte, Dir, BSG, Dr Arun Sharma, Head, FTD and Shri G Ganesh, Head, TT&CD



Dr S Basu, Director, BARC, addressing the group during transfer of technology to M/s SCRIMAD.

growers of Madagascar with Mr.Simon Rakotondrahova, GM, M/s SCRIMAD. Dr.S.K. Apte, Director, Bioscience Group; Dr. A. K. Sharma, Head, FTD, and Shri G Ganesh, Head, Technology Transfer & Collaboration Division, too were present during this technology transfer. Later, the technology was demonstrated to Mr.Simon Rakotondrahova by processing the fresh fruit at FTD, BARC. He was also given sample fruits which were processed about 10 days back for taste and he was fully satisfied.

F. "Auto TLD Badge Reader" technology was transferred to M/s. Intech Dosimeters Pvt. Ltd., New Delhi on 22/08/2014.

PC based automatic TLD badge reader (Auto-TLD BR) has been developed by RP&AD to ensure health and safety of persons working in radiation environment by monitoring the radiation dose received by them (as per the TLD badges worn by them) and maintain a record. The Auto-TLD BR (Model TLDBR 7B) is capable of automatically



Standing from right are :Sh. R.N Khanderao,, Dr Ratna Pradeep, Head,TLD PMSS, RP&AD, Sh. V.N Kabadi, Director, M/s. Intech Dosimeters Pvt. Ltd., Sh. G.Ganesh, Head, TT&CD, Dr. D.A.R Babu, Head, RP&AD, Dr. M.S Kulkarni, Head, RPIS, RP&AD and Smt. Preeti K Pal, TT&CD

evaluating 50 TLD badges. It has built-in diagnostic software & safeguards against malfunctioning. This badge reader finds its application in the Personnel Monitoring of radiation workers in Nuclear power stations, Isotope laboratories, Industrial radiography installations, diagnostic & therapeutic radiology centres, etc.

G."Nitrogen Oxides releasing wound dressing" technology was transferred to M/s Cologenes Healthcare Pvt. Ltd., Salem (T.N.) on September 15th, 2014.

The technology of "Nitrogen Oxides releasing wound dressing" has been developed by Water and Steam Chemistry Division, BARC Facilities, Kalpakkam under technology incubation MoU with M/s Cologenes Healthcare Pvt. Ltd., Salem (T.N.). The dressing works on the principle of release of gaseous nitrogen oxides (including nitric oxide) from a collagen matrix containing citric acid and sodium nitrite. The hydrogel based dressing possesses the antimicrobial properties of acidified sodium nitrite and the properties of collagen such as attraction of keratinocytes and fibroblasts to the wound area that encourages angiogenesis and re-epithelialization. The cotton gauze-collagen hydrogel combination is



Photograph after signing the agreement with M/s Cologenes Healthcare Pvt. Ltd., Salem (T.N.), seen from left to right, Dr. B. N. Jagtap, Director, ChG, Shri R. Krishna Kumar, MD, M/s Cologenes Healthcare Pvt. Ltd., Shri G. Ganesh, Head, TT&CD, Dr. V. P. Venugopalan, Head, BBPS, WSCD & Shri V. K. Upadhyay, TT&CD.

cross-linked by glutaraldehyde and dried by freeze-drying. At the time of application, the freeze-dried dressing is wetted by sodium nitrite solution.

The nitrogen oxides releasing wound dressing is useful for treatment of chronic infected wounds and non-healing wounds (diabetic foot, pressure ulcer, venous stasis wound etc). The dressing works by decreasing the infection, increasing the microvascularization and granulation thereby aiding faster wound healing. The dressing is also suitable for application which requires preparation of wound bed for acceptance of split skin graft based surgery.

H.Nisargruna Biogas Technology based on biodegradable waste has been developed by NA&BTD. The plant processes biodegradable waste into biogas and weed free manure. It was transferred to the following nine parties :-

- M/s Venson Green Solutions Pvt. Ltd., Mysore on 11.4.2014
- M/s Innovative Environmental Technologies Pvt. Ltd., Pune on 21.4.2014

- M/s. North East Green Tech Pvt. Ltd., Assam on 29.5.2014
- M/s. Green & Clean Solutions (P) Ltd., Bangalore on 25.6.2014
- M/s. Synod Bioscience Pvt. Ltd., Cochin on 21.7.2014
- M/s. Engynova Technologies, Navi Mumbai on 31.7.2014
- M/s. VIMI Associates, Latur on 18.8.2014
- M/s. PCP Chemicals Pvt. Ltd., Thane on 8.9.2014
- M/s. Ajna Advisors Pvt. Ltd., Mumbai on 24.9.2014

Honour for BARC

The Plant Mutation Breeding Team, Nuclear Agriculture & Biotechnology Division, BARC received the "Achievement Award" instituted by the Joint FAO/IAEA Programme on Nuclear Techniques in Food and Agriculture. This award was received by Dr. Sekhar Basu, Director, BARC in Vienna, in September 2014 and was given in appreciation and recognition of the contribution to food security and sustainable agricultural development through Plant Mutation Breeding



Dr. Sekhar Basu, Director, BARC receiving the Achievement Award from Mr. Aldo Malawasi, Deputy Director General of the IAEA Dept. of Nuclear Applications (DDG-NA) and Mr. Deepak Ojha, Counsellor, Atomic Energy Permanent Mission of India

BARC Scientists Honoured

Name of the Scientist : **S.M. Yusuf**
Affiliation : Solid State Physics Division
Award/Honour : Elected as a Fellow of the National Academy of Sciences, India in the year 2014

Name of the Scientists : **N.S.Rawat, M.S.Kulkarni,D.R.Mishra, B.C.Bhatt and D.A.R.Babu**
Affiliation : Radiological Physics & Advisory Division
Award/Honour : Best poster paper award
Title of the Paper : An attempt to correlate shift in TL peak with heating rate and black-body radiation
Presented at : 31th National Conference on Advances in Radiation Measurement Systems and Techniques; organized by the Indian Association for Radiation Protection (IARP) and held at BARC, Mumbai during March 19-21, 2014.



Central Complex, BARC

Edited & Published by:
Scientific Information Resource Division,
Bhabha Atomic Research Centre, Trombay, Mumbai 400 085, India
BARC Newsletter is also available at URL:<http://www.barc.gov.in>